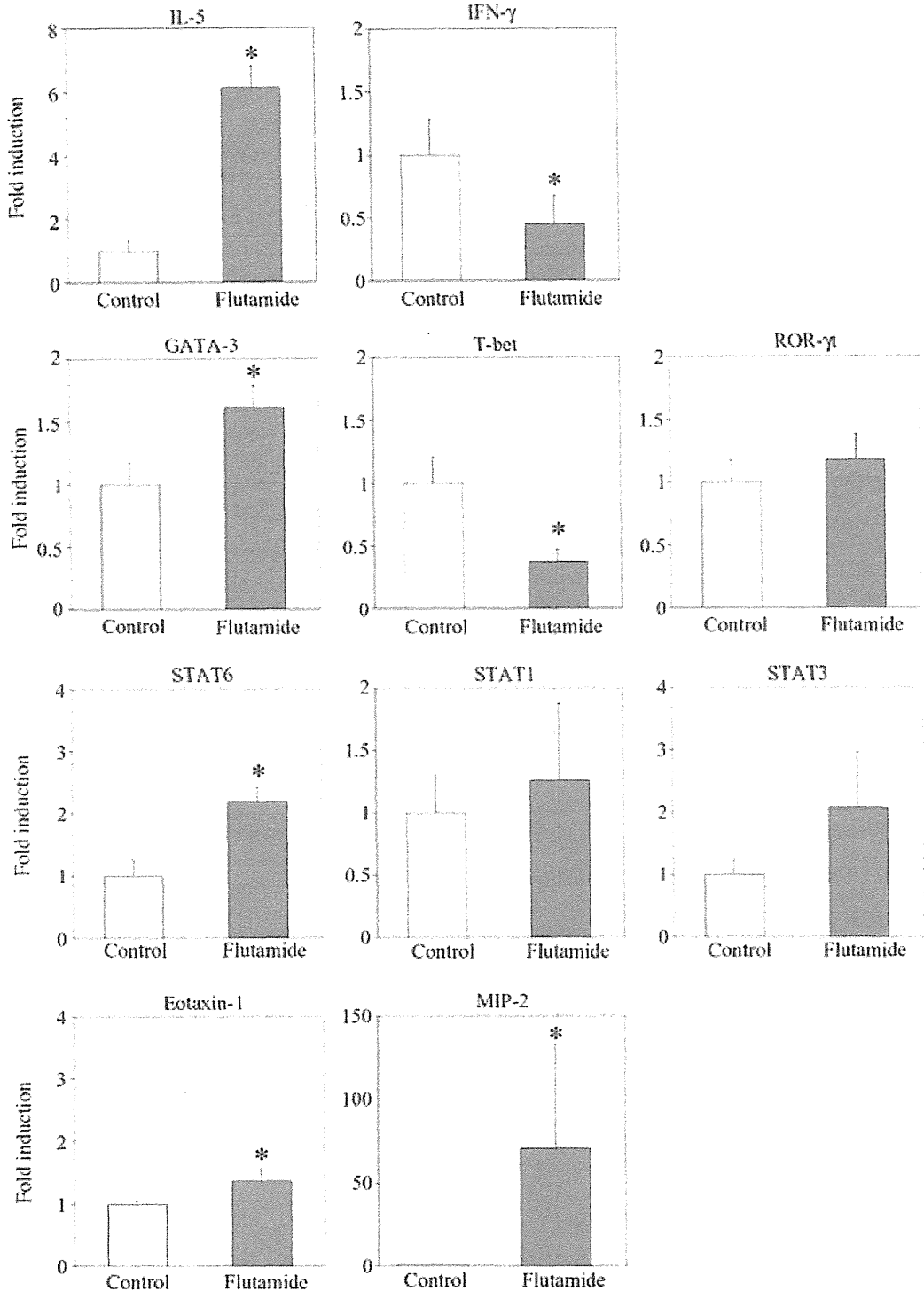

Figure 2. Hepatic mRNA levels of transcriptional factors, cytokines and chemokines in flutamide-administered mice. Flutamide was orally administered at a dose of 1500 mg/kg and mRNA levels of T-bet, GATA-3, ROR-gt, IFN-g, IL-5, STAT6, STAT1, STAT3, Eotaxin-1, and MIP-2 in the liver were measured by real time RT-PCR 6 h after the administration. Data are mean ± SD (n = 4). Significantly different from control mice (*$p < 0.05$).

involved in the flutamide-induced liver injury, we measured plasma IL-4 in flutamide-administered mice (Fig. 3A). The plasma IL-4 level was significantly increased in flutamide-administered mice compared with control mice. In nontreated control mice, plasma IL-4 was not detected. To further investigate whether IL-4 was involved in the flutamide-induced liver injury, we performed IL-4 neutralization studies (Fig.3B). The i.p. administration of anti-mouse IL-4 antibody significantly reduced the plasma ALT, but rat IgG2a treatment demonstrated no effect on the flutamide-induced liver injury.

Journal of AppliedToxicology

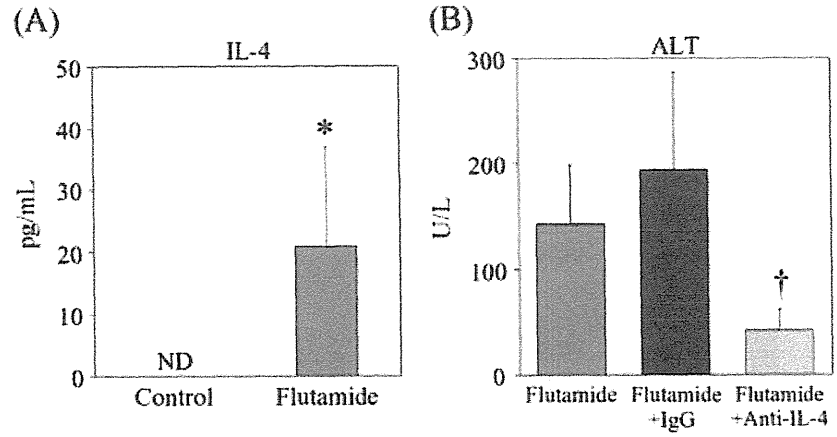

Figure 3. PlasmaIL-4 level and effects of anti-mouse IL-4 antibody administration on plasma ALT in flutamide-administered mice. Flutamide was orally administered at a dose of 1500 mg/kg, and plasma IL-4 level was measured by ELISA 6 h after the administration (A). Anti-mouse IL-4 antibody (0.1 mg/mouse, i.p.) was administered one hour before the flutamide administration. Plasma ALT levels were measured 6 h after the flutamide administration (B). Data are mean ± SD (n = 4). Significantly different from control mice (*$p < 0.05$); significantly different from flutamide-plus control IgG2a-administered group (†$p < 0.05$).

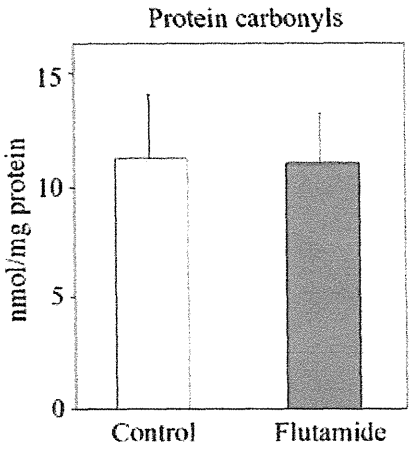

Figure 4. Protein carbonyl level in flutamide-administered mice. Flutamide was orally administered at a dose of 1500 mg/kg. The plasma protein carbonyl level was measured 6 h after the administration. Data are mean ± SD (n = 4). Significantly different from control mice (*$p < 0.05$).

Protein Carbonyl Level in Flutamide-administered Mice

It has been reported that oxidative stress is involved in flutamide-induced liver injury (Kashimshetty *et al.*, 2009; Yoshikawa *et al.*, 2009b). Then, we measured protein carbonyl, which is a general biomarker for oxidative stress (Davies, 1987). The protein carbonyl level in plasma was not changed in flutamide-administered mice, compared with control mice (Fig. 4). This result suggested that oxidative stress is not likely to be involved in this flutamide-induced liver injury model.

Effects of DK-PGD_2 Treatment on Flutamide-induced Liver Injury

We previously demonstrated the effects of the DK-PGD_2, a selective CRTh2 agonist, on dicloxacillin-induced liver injury. The DK-PGD_2 administration exacerbated dicloxacacllin-induced liver injury (Higuchi *et al.*, 2011). We investigated the effects of DK-PGD_2 on flutamide-induced liver injury. The plasma ALT level was significantly increased in flutamide/DK-PGD_2-cotreated mice, compared with flutamide-administered mice (Fig. 5A). DK-PGD_2 administration alone had no effects on the plasma ALT level. This set of mice was different from that which was used in Figs 1–4. In the histopathological study, a few infiltrating mononuclear cells were observed in flutamide-administered mice, whereas spotty necrosis and mononuclear cells infiltration were observed in flutamide/DK-PGD_2-cotreated mice (Fig. 5B).

Effects of DK-PGD_2 Treatment on Plasma IL-4 Level and Hepatic mRNA Expressions

To investigate the underlying mechanisms responsible for the increased susceptibility of DK-PGD_2 treated mice to flutamide-induced liver injury, the plasma IL-4 level and hepatic mRNA expressions were measured. The plasma IL-4 level was significantly increased in flutamide/DK-PGD_2-cotreated mice compared with flutamide-administered mice. The hepatic mRNA levels of GATA-3 and MIP-2 were significantly increased compared with flutamide-administered mice (Fig. 5C). In particular, MIP-2 mRNA was markedly increased 200-fold compared with nontreated control. In contrast, the expressions of IFN-γ, IL-5, T-bet, ROR-γt, and Eotaxin-1 mRNA were not changed (data not shown). These results suggested that Th2 cytokines are mainly involved in the exacerbation of flutamide-induced hepatotoxicity by DK-PGD_2.

DISCUSSION

Previous studies demonstrated that a high dose of flutamide (500 mg kg^{-1}, daily for 3 days by oral gavage) caused an increase of the liver–body weight ratio, but no increase in the serum ALT level in rat (Coe *et al.*, 2006), and repeated high doses of flutamide (400 mg kg^{-1}, daily for 28 days) did not cause an increase in the plasma ALT level in SV129 mouse (Matsuzaki *et al.*, 2006). Thus, these reports suggested that it is difficult to induce flutamide-induced liver injury at repeated high doses in rodents. After testing many different conditions for flutamide

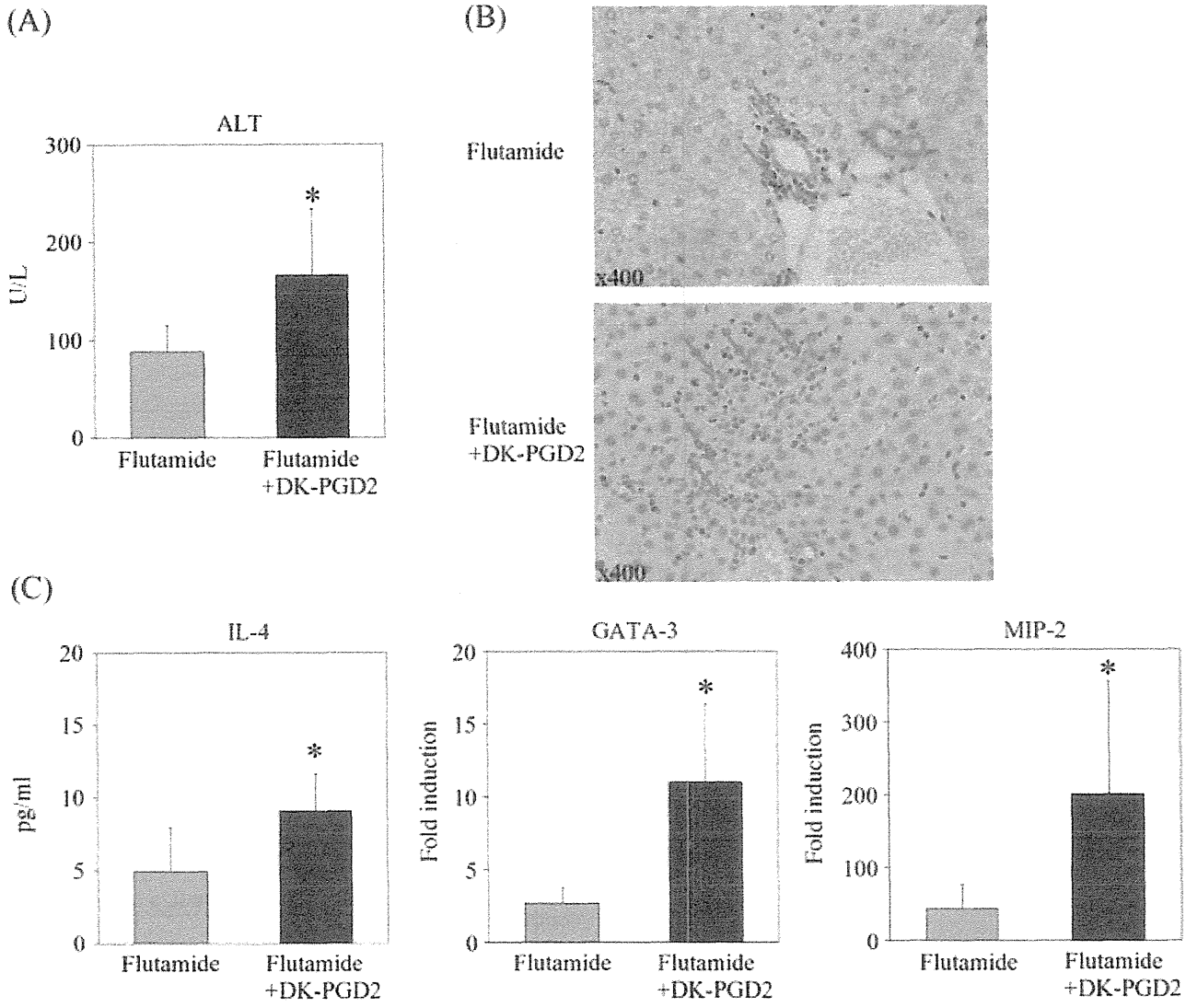

Figure 5. Effects of DK-PGD_2 treatment on flutamide-induced liver injury in mice. Flutamide was orally administered at a dose of 1500 mg/kg. The plasma ALT level was measured 6 h after the administration. DK-PGD_2 (10 μg/mouse, i.p.) was administered 1 h after the flutamide administration (A). Liver specimens were prepared 6 h after the flutamide administration. Liver tissue sections were stained with H&E (B). Arrows indicate necrotic cells with infiltration of neutrophils. Plasma IL-4 level was measured by ELISA and hepatic GATA-3 and MIP-2 mRNA levels were measured by real time RT-PCR (C). Data are mean ± SD (n = 5 for flutamide, 7 for flutamide + DK-PGD_2). Significantly different from flutamide-administered mice (*$p < 0.05$).

adminitration in mice, finally, we found that administration of flutamide (1500 mg kg^{-1}, single, p.o.) in a nonfasting condition causes flutamide-induced acute hepatotoxicity in mice.

The plasma ALT and AST levels were significantly increased in flutamide-administered mice after 3, 6 and 9 h compared with control mice, and were attenuated by 24 h (Fig. 1). In the present study, we investigated the involvement of immunological factors in flutamide-induced liver injury. The administration of flutamide significantly increased the expression of IL-5, GATA-3, STAT6 and Eotaxin-1. These results suggested that Th2-immune factors would be involved in flutamide-induced liver injury in BALB/c mice, and the plasma IL-4 level was significantly increased in flutamide-administered mice. In addition, neutralization of IL-4 suppressed the hepatotoxicity of flutamide. IL-4 plays a central role in Th2-dominant responses and activates STAT6 and GATA-3, which induce IL-5 and Eotaxin (Agnello *et al.*, 2003; Jaruga *et al.*, 2003), and IL-5 and Eotaxin-1 play roles in development and accumulation of eosinophils and basophils, followed by allergic inflammation (Kay, 2001). In addition, it has been reported that the plasma IL-4 levels were elevated in patients with liver injury of various kinds (Spanakis *et al.*, 2002; Harada *et al.*, 1997). Thus, more investigations are needed into whether IL-4 might be involved the pathogenesis of many DILI. MIP-2 mRNA expression was remarkably increased in flutamide-administered mice. MIP-2 is mainly secreted from macrophages and plays a role in neutrophil accumulation; halothane administration also greatly increases MIP-2 mRNA expression in BALB/c mice (Jaeschke and Hasegawa 2006; Kobayashi *et al.*, 2009). MIP-2, followed by mononuclear cell migration into the liver, might be involved in the flutamide hepatotoxicity.

We demonstrated that IL-4 is involved in flutamide hepatotoxicity by the administration of anti-IL-4 monoclonal antibody

(Fig. 3B). In general, IL-4- or IL-5-deficient mice were suggested to be useful for the investigation of allergic mechanisms for IL-4 or IL-5 (Hogan *et al.*, 1998). However, cytokines markedly change hepatic P450 expressions (Abdel-Razzak *et al.*, 1993). Since flutamide is metabolized by various CYPs (Matsuzaki *et al.*, 2006; Ohbuchi *et al.*, 2009), changes in the expression of drug metabolizing enzymes should be carefully pre-evaluated using IL-4 or IL-5 knockout mouse. Thus, we did not use knockout mouse in the present study.

Next, we investigated the effects of oxidative stress on flutamide-induced liver injury. Flutamide is known as an inhibitor of complex I of mitochondria, and inhibition of complex I leads to increased levels of superoxide, which induce oxidative stress (Fau *et al.*, 1994). In an *in vivo* study, a heterozygous deficiency of superoxide dismutase 2 (SOD2) and the depletion of glutathione, which serves an important function in protecting tissues against oxidative damage, exacerbated flutamide hepatotoxicity in mouse (Kashimshetty *et al.*, 2009) and rat (Morita *et al.*, 2009). These reports suggested that oxidative stress was involved in flutamide-induced liver injury. Therefore, we analyzed the protein carbonyl level, which is widely used as an oxidative stress marker (Davies, 1987). The protein carbonyl level was not changed in flutamide-administered mice. This result suggested that oxidative stress is not likely to be involved in flutamide-induced liver injury in BALB/c mice.

CRTh2, one of the PGD_2 receptors, plays a major role in atopic dermatitis, allergic asthma and airway inflammation, and it was demonstrated that CRTh2 is responsible for PGD_2 chemotaxis of Th2 cells, eosinophils, basophils and monocytes (Kostenis and Ulven, 2006). DK-PGD_2, a CRTh2-selective agonist, enhances Th2-type inflammation (Spik *et al.*, 2005). In a previous study, we demonstrated that DK-PGD_2 administration exacerbated dicloxacillin-induced liver injury in mouse, which involved Th2 immune factors such as IL-4 and Eotaxin (Higuchi *et al.*, 2011). We hypothesized that DK-PGD_2 may exacerbate flutamide-induced liver injury. To examine this hypothesis, BALB/c mice were cotreated with flutamide and DK-PGD_2. The plasma ALT and IL-4 levels were significantly increased in flutamide/DK-PGD_2-cotreated mice compared with flutamide-administered mice, which supported the involvement of Th2 factors. The plasma IL-4 level in flutamide-administered mice was higher in Fig. 3 than in Fig. 5(C), but it was not significant. The experimental conditions were the same. In this study, mice were administered orally flutamide in nonfasting condition, and the stomach content might affect flutamide absorption, resulting in the difference in IL-4 levels.

In the histopathological study, spotty necrosis and mononuclear cell infiltration were observed in flutamide/DK-PGD_2-cotreated mice (Fig. 5B). It has been reported that flutamide activates neutrophil accumulation (Srinivasan *et al.*, 1997), and MIP-2 mRNA expression was remarkably increased in flutamide/DK-PGD_2-cotreated mice (Fig. 5C), and was followed by the infiltration of mononuclear cells into the liver. Compared with our previous dicloxacillin study, the expression levels of Eotaxin-1 and monocyte chemoattractant protein-1 mRNA were not changed in flutamide/DK-PGD_2-cotreated mice, which might be due to differences in the IL-4 secretion level induced by flutamide and dicloxacillin. Th2 immune factors-mediated liver injury was exacerbated by DK-PGD_2, which could be a novel method to detect hepatotoxicity of new compounds in drug development.

In conclusion, we reported for the first time that immunological factors are involved in flutamide-induced liver injury in mice, and that DK-PGD_2 could be useful for the detection of Th2 immune factors that mediate liver injury. The present study may shed light on the mechanisms of DILI.

Acknowledgments

We thank Mr Brent Bell for reviewing the manuscript. This work was supported by Health and Labor Sciences Research Grants from the Ministry of Health, Labor and Welfare of Japan (H20-BIO-G001).

REFERENCES

Abdel-Razzak Z, Loyer P, Fautrel A, Gautier JC, Corcos L, Turlin B, Beaune P, Guillouzo A. 1993. Cytokines down-regulate expression of major cytochrome P-450 enzymes in adult human hepatocytes in primary culture. *Mol. Pharmacol.* **44**: 707–715.

Agnello D, Lankford CS, Bream J, Morinobu A, Gadina M, O'Shea JJ, Frucht DM. 2003. Cytokines and transcription factors that regulate T helper cell differentiation: new players and new insights. *J. Clin. Immunol.* **23**: 147–161.

Biedermann BT, Knelling M, Mailhammer R, Maier K, Sander CA, Kollias G, Kunkel S L, Hultner L, Rocken M. 2000. Mast cell control neutrophil recruitment during T cell-mediated delayed hypersensitivity reactions through tumor necrosis factor and macrophage inflammatory protein 2. *J. Exp. Med.* **192**: 1441–1451.

Coe KJ, Nelson SD, Ulrich RG, He Y, Dai X, Cheng O, Caguyoung M, Roberts CJ, Slatter JG. 2006. Profiling the hepatic effects of flutamide in rats: a microarray comparison with classical aryl hydrocarbon receptor ligands and atypical Cyp1a inducers. *Drug Metab. Dispos.* **34**: 1266–1275; doi: 10.1124/dmd.105.009159.

Davies KJA. 1987. Protein damage and degradation by oxygen radicals. *J. Biol. Chem.* **262**: 9895–9901.

Dourakis SP, Alexopoulou AA, Hadziyannis SJ. 1994. Fulminant hepatitis after flutamide treatment. *J. Hepatol.* **20**: 350–353.

Fau D, Eugene D, Berson A, Letteron P, Fromenty B, Fisch C, Pessayre D. 1994. Toxicity of the antiandrogen flutamide in isolated rat hepatocytes. *J. Pharmacol. Exp. Ther.* **269**: 954–962.

Gomez J, Dupont A, Cuan L, Tremblay M, Suburu R, Lemay M, Labrie, F. 1992. Incidence of liver toxicity associated with the use of flutamide in prostate cancer patients. *Am. J. Med.* **92**: 465–470.

Harada K, Water JV, Leung PSC, Coppel RL, Ansari A, Nakanuma Y, Gershwin ME. 1997. In situ nucleic acid hybridization of cytokines in primary biliary cirrhosis: predominance of the Th1 subset. *Hepatology* **25**: 791–796; doi: 10.1002/hep.510250402.

Hart W, Stricker BHC. 1989. Flutamide and hepatitis. *Ann. Intern. Med.* **110**: 943–944.

Heneghan MA, McFarlane IG. 2002. Current and novel immunosuppressive therapy for autoimmune hepatitis. *Hepatology* **35**: 7–13; doi: 10.1053/jhep.2002.30991.

Higuchi S, Kobayashi M, Yoshikawa Y, Tsuneyama K, Fukami T, Nakajima M, Yokoi T. 2011. IL-4 mediates dicloxacillin-induced liver injury in mice. *Toxicol. Lett.* **200**: 139–145; doi: 10.1016/j.toxlet.2010.11.006.

Hogan SP, Matthaei KI, Young JM, Koskinen A, Young IG, Foster PS. 1998. A novel T cell-regulated mechanism modulating allergen-induced airways hyperreactivity in BALB/c mice independently of IL-4 and IL-5. **161**: 1501–1509.

Holt MP, Ju C. 2006. Mechanisms of drug-induced liver injury. *AAPS J.* **8**: E48–E54; doi: 10.1208/aapsj080106.

Jaeschke H, Hasegawa T. 2006. Role of neutrophils in acute inflammatory liver injury. *Liver Int.* **26**: 912–919; doi: 10.1111/j.1478-3231.2006.01327.x.

Jaruga B, Hong F, Sun R, Radaeva S, Gao B. 2003. Crucial role of IL-4/STAT6 in T cell-mediated hepatitis: up-regulating eotaxins and IL-5 and recruiting leukoctyes. *J. Immunol.* **171**: 3233–3244.

Kashimshetty R, Desai VG, Kale VM, Lee T, Moland CL, Branham WS, New LS, Chan ECY, Younis H, Boelsterli UA. 2009. Underlying mitochondrial dysfunction triggers flutamide-induced oxidative liver injury in a mouse model of idiosyncratic drug toxicity. *Toxicol. Appl. Pharmacol.* **238**: 150–159; doi: 10.1016/j.taap.2009.05.007.

Kay AB. 2001. Allergy and allergic diseases. *New Engl. J. Med.* **344**: 30–37; doi: 10.1056/NEJM200101043440106.

Kidd P. 2003. Th1/Th2 balance: the hypothesis, its limitations, and implications for health and disease. *Altern. Med. Rev.* **8**: 223–246.

Kita H, Macky IR, Van DWJ, Gershwin ME. 2001. The lymphoid liver: considerations on pathways to autoimmune injury. *Gastroenterology* **120**: 1485–1501.

Kobayashi E, Kobayashi M, Tsuneyama K, Fukami T, Nakajima M, Yokoi T. 2009. Halothane-induced liver injury is mediated by interleukin-17 in mice. *Toxicol. Sci.* **111**: 302–310; doi: 10.1093/toxsci/kfp165.

Kostenis E, Ulven T. 2006. Emerging roles of DP and CRTh2 in allergic inflammation. *Trends Mol. Med.* **12**: 148–158; doi: 10.1016/j.molmed.2006.02.005.

Leonard WJ, O'Shea JJ. 1998. Jaks and STATs: biological implications. *Annu. Rev. Immunol.* **16**: 293–322; doi: 10.1146/annurev.immunol.16.1.293.

Matsuzaki Y, Nagai D, Ichimura E, Goda R, Tomura A, Doi M, Nishikawa K. 2006. Metabolism and hepatic toxicity of flutamide in cytochrome P450 1A2 knockout SV129 mice. *J. Gastroenterol.* **41**: 231–239; doi: 10.1007/s00535-005-1749-y.

Moller S, Iversen P, Franzmann MB. 1990. Flutamide-induced liver failure. *J. Hepatol.* **10**: 346–349.

Montgomery RA, Dallman MJ. 1991. Analysis of cytokine gene expression during fetal thymic ontogeny using the polymerase chain reaction. *J. Immunol.* **147**: 554–560.

Morita M, Akai S, Hosomi H, Tsuneyama K, Nakajima M, Yokoi T. 2009. Drug-induced hepatotoxicity test using γ-glutamylcysteine synthetase knockdown rat. *Toxicol. Lett.* **189**: 159–165; doi:10.1016/j.toxlet.2009.05.016.

Ohbuchi M, Miyata M, Nagai D, Shimada M, Yoshinari K, Yamazoe Y. 2009. Role of enzymatic N-hydroxylation and reduction in flutamide metabolite-induced liver toxicity. *Drug Metab. Dispos.* **37**: 97–105; doi: 10.1124/dmd.108.021964.

Spanakis NE, Garinis GA, Alexopoulos EC, Patrinos GP, Menounos PG, Sklavounou A, Manolis NE, Gorgoulis VG, Valis D. 2002. Cytokines serum levels in patients with chronic HCV infection. *J. Clin. Lab. Anal.* **16**: 40–46.

Spik I, Brenuchon C, Angeli V, Staumont D, Fleury S, Capron M, Trottein F, Dombrowicz D. 2005. Activation of the prostaglandin D2 receptor DP2/CRTH2 increases allergic inflammation in mouse. *J. Immunol.* **174**: 3703–3708.

Srinivasan R, Buchweitz JP, Ganey PE. 1997. Alteration by flutamide of neutrophil response to stimulation. Implications for tissue injury. *Biochem. Pharmacol.* **53**: 1179–1185.

Steinman L. 2007. A brief history of Th17, the first major revision in the Th1/Th2 hypothesis if T cell-mediated tissue damage. *Nat. Rev. Med.* **13**: 139–145; doi: 10.1038/nm1551.

Takeshita K, Yamasaki T, Nagano K, Sugimoto H, Shichijo M, Gantner F, Bacon BK. 2004. CRTH2 is a prominent effector in contact hypersensitivity-induced neutrophil inflammation. *Int. Immunol.* **16**: 947–959; doi: 10.1093/intimm/dxh096.

Watanabe A, Fukami T, Nakajima M, Takamiya M, Aoki Y, Yokoi T. 2010. Human arylacetamide deacetylase is a principal enzyme in flutamide hydrosis. *Drug Metab. Dispos.* **37**: 1513–1520; doi: 10.1124/dmd.110.033720.

Wysowski DK, Fourcroy JL. 1996. Flutamide hepatotoxicity. *J. Urol.* **155**: 209–212.

Wysowski DK, Freiman JP, Tourtelot JB 1993. Fatal and nonfatal hepatotoxicity associated with flutamide. *Ann. Intern. Med.* **118**: 860–864.

Yoshikawa Y, Morita M, Hosomi H, Tsuneyama K, Fukami T, Nakajima M, Yokoi T. 2009a. Knockdown of superoxide disumutase 2 enhances acetaminophen-induced hepatotoxicity in rat. *Toxicology* **264**: 89–95; doi: 10.1016/j.tox.2009.07.017.

Yoshikawa Y, Hosiomi H, Fukami T, Nakajima M, Yokoi T. 2009b. Establishment of knockdown of superoxide dismutase 2 and expression of CYP3A4 cell system to evaluate drug-induced cytotoxicity. *Toxicol. in Vitro* **23**: 1179–1187; doi: 10.1016/j.tiv.2009.05.024.

Arch Toxicol (2011) 85:199–207
DOI 10.1007/s00204-010-0584-y

MOLECULAR TOXICOLOGY

Stimulation of pro-inflammatory responses by mebendazole in human monocytic THP-1 cells through an ERK signaling pathway

Katsuhiko Mizuno · Yasuyuki Toyoda · Tatsuki Fukami · Miki Nakajima · Tsuyoshi Yokoi

Received: 8 June 2010 / Accepted: 1 September 2010 / Published online: 17 September 2010

Abstract Oral helminthic mebendazole (MBZ) has been reported to cause liver injury with inflammatory responses. However, the underlying mechanism remains unknown. To examine the inflammatory reactions, we investigated whether MBZ and other helminthic drugs increase the release of pro-inflammatory cytokines and chemokines using human monocytic cells. The release of interleukin (IL)-8 and tumor necrosis factor (TNF) α from human monocytic THP-1 cells was significantly increased by treatment with MBZ, albendazole (ABZ), fenbendazole (FBZ), or oxibendazole (OBZ), but not by albendazole sulfoxide or praziquantel, suggesting that MBZ and structurally similar drugs can stimulate monocytes and increase the release of pro-inflammatory cytokines. MBZ also significantly increased the phosphorylation of extracellular signal-regulated kinase (ERK) 1/2 and c-Jun N-terminal kinase (JNK) 1/2 in THP-1 cells. Pretreatment with the MAP kinase/ERK kinase 1/2 inhibitor U0126 significantly suppressed the increase of IL-8 and TNFα levels by MBZ, ABZ, FBZ, or OBZ treatment in THP-1 cells, but the p38 mitogen-activated protein kinase inhibitor SB203580 or JNK1/2 inhibitor SP600125 did not. These results suggested that an ERK1/2 pathway plays an important role in the release of IL-8 and TNFα in THP-1 cells treated with MBZ and structurally similar drugs. In conclusion, the release of inflammatory mediators by MBZ might be one of the mechanisms underlying immune-mediated liver injury. This in vitro method may be useful to predict adverse inflammatory reactions that lead to hepatotoxicity.

Keywords Mebendazole · THP-1 cell · Hepatotoxicity · IL-8 · TNFα

K. Mizuno · Y. Toyoda · T. Fukami · M. Nakajima · T. Yokoi (✉)
Drug Metabolism and Toxicology, Faculty of Pharmaceutical Sciences, Kanazawa University, Kakuma-machi, Kanazawa 920-1192, Japan
e-mail: tyokoi@kenroku.kanazawa-u.ac.jp

Introduction

Drug-induced liver injury is the most frequent reason for the withdrawal of an approved drug from the market and for failures in drug development in pharmaceutical companies. Because of significant adverse drug reactions associated with hepatotoxicity, several drugs have been removed from the pharmaceutical market (Holt and Ju, 2006). Inflammatory stress might be caused by xenobiotics or drugs leading to idiosyncratic adverse drug reactions. The sporadic occurrence of acute inflammatory episodes could explain the onset of some idiosyncratic reactions during clinical drug therapy (Ganey et al. 2004; Roth et al. 2003; Tafazoli et al. 2005). Inflammatory reactions in liver are induced by the activation of immune cells, such as monocytes, macrophages and Kupffer cells. Activated monocytes and macrophages release large amounts of pro-inflammatory cytokines and chemokines, including interleukin (IL)-1, tumor necrosis factor (TNF) α, and IL-8. TNFα triggers the release of a cascade of other cytokines and recruits activated immune cells, including lymphocytes and macrophages (Bradham et al. 1998). IL-8 exhibits multiple effects on neutrophils, including the induction of lysosomal enzyme release, the increase in the expression of adhesion molecules, and rapid infiltration (Leonard et al. 1991; Baggiolini et al. 1994). In several rodent models, it was shown that the production of TNFα and neurtophil infiltration in liver play a critical role in immune-mediated

liver injury by drugs such as acetaminophen, non-steroidal anti-inflammatory drugs, and antibiotics (Jaeschke 2005; Deng et al. 2009).

Recently, it has been reported that human monocytic cell lines were useful to examine the inflammatory responses mediated by drugs withdrawn from the market. In human monocytic THP-1 cells, the mRNA expression levels and/or the release of pro-inflammatory cytokines and chemokines were increased by the treatment with troglitazone or ximelagatran (Edling et al. 2008, 2009).

Many benzimidazoles have been launched on the market and used in clinical drug therapy. Mebendazole (MBZ) and other structurally related drugs are used for the therapy of various helminthic infections as well as for the treatment of hydatid disease and alveolar echinococcosis (Ammann and Eckert 1996). However, MBZ has been reported to cause hepatic injury. Bekhti and Pirotte (1987) described a case of acute hepatocellular injury in a patient treated with MBZ 600 mg/day for echinococcosis. Colle et al. (1999) reported a case of granulomatous hepatitis with eosinophilia after the administration of MBZ. Seitz et al. (1983) and Junge and Mohr (1983) reported MBZ-induced hepatic injury, and the liver biopsy of the patient revealed hepatocytic necrosis and portal inflammation with eosinophils during long-term (49–60 days) and high-dose (2–3.5 g/day) therapy with MBZ. Recently, MBZ has been carefully used in clinical drug therapy, thus case reports of severe hepatic injury are very rare (Bagheri et al. 2004). Chen et al. (2003) reported that MBZ is associated with Steven-Johnson syndrome (SJS)/toxic epidermal necrolysis (TEN), suggesting the involvement of immune-mediated factors. However, the mechanism underlying the hepatic injury by MBZ remains to be clarified.

Considering the case reports of hepatic injury by MBZ, we hypothesized that benzimidazoles stimulate inflammatory responses that may result in immune-mediated hepatic injury. The purpose of this study is to investigate whether benzimidazoles stimulate the release of pro-inflammatory cytokines and chemokines from human monocytic cells and to clarify the involvement of cell signaling in the release of pro-inflammatory cytokines and chemokines from THP-1 cells.

Materials and methods

Materials

ABZ, fenbendazole (FBZ), MBZ, oxibendazole (OBZ), and praziquantel (PZQ) were purchased from Sigma–Aldrich (St. Louis, MO). Albendazole sulfoxide (ABZSO) was purchased from Toronto Reserch Chemicals (Ontario, Canada). Lipopolysaccharide (LPS) was also from Sigma–Aldrich (St. Louis, MO). Primers were commercially synthesized at Hokkaido System Sciences (Sapporo, Japan). The monoclonal antibodies of anti-Thr202/Tyr204 phosphorylated extracellular signal-regulated kinase (ERK) 1/2, anti-Thr180/Tyr182 phosphorylated p38 mitogen-activated protein (MAP) kinase, and anti-Thr183/Tyr185 phosphorylated c-Jun N-terminal kinase (JNK) 1/2 were purchased from Cell Signaling Technology (Beverly, MA). The monoclonal antibodies against ERK1/2 and JNK1/2 and the polyclonal antibody against p38 MAP kinase were also from Cell Signaling Technology. All other reagents were of the highest grade commercially available.

Cell culture

The human monocytic leukemia cell line THP-1 was obtained from Riken Gene Bank (Tsukuba, Japan). HL-60 and KG-1 cells were obtained from American Type Culture Collection (Manassas, VA). THP-1 cells were cultured in RPMI 1640 medium (Nissui Pharmaceutical, Tokyo, Japan) supplemented with 10% fetal bovine serum (FBS; Invitrogen, Carlsbad, CA). HL-60 and KG-1 cells were cultured in RPMI 1640 medium supplemented with 20% FBS. These cells were maintained at 37°C under an atmosphere of 5% CO_2.

Drug treatment of human monocytic cell lines

THP-1, HL-60, and KG-1 cells were seeded at a density of 1×10^6 cells/well in 24-well plates with the medium containing the indicated concentration of helminthic drugs, and then incubated at 37°C. The final concentration of dimethyl sulfoxide (DMSO) in medium was 0.1%. In experiments using MAP kinase inhibitors, cells were pretreated with MAP kinase/ERK kinase (MEK) 1/2 inhibitor U0126 (Wako Pure Chemical Industries), p38 MAP kinase inhibitor SB203580 (Wako Pure Chemical Industries), or JNK1/2 inhibitor SP600125 (Calbiochem, Los Angeles, CA) for 1 h, and then treated with the helminthic drugs. Supernatants were separated from cell cultures by centrifugation and stored at −70°C until assayed. For immunoblot analysis, the cells were suspended in TGE buffer (10 mM Tris–HCl, 20% glycerol, 1 mM EDTA, pH 7.4) and disrupted by freeze-thawing three times.

Enzyme-linked immunosorbent assay (ELISA)

The pro-inflammatory cytokine TNFα and the chemokine IL-8 in cell supernatants were measured by Human TNFα and IL-8 ELISA Ready-SET-GO!™ (eBioscience, San Diego, CA) according to the manufacturer's instructions.

Real-time reverse transcription-polymerase chain reaction (RT–PCR)

Total RNA was extracted from THP-1 cells with RNAiso (Takara Bio, Shiga, Japan) according to the protocol supplied by the manufacturer. Reverse transcription was performed with ReverTra Ace (Toyobo, Tokyo, Japan) according to the manufacturer's protocol. For quantitative analysis, real-time RT–PCR was performed for inflammatory cytokine mRNA using an MX3000P real-time PCR system (Stratagene, La Jolla, CA). The primers used in this study were human IL-8 (forward: 5′-CAGCCTTCCTG ATTTCTCTGCAG-3′, reverse: 5′-AGACAGAGCTCTC TTCCATCAG-3′) and human TNFα (forward: 5′-CTT CTGCCTGCTGCACTTTGGAG-3′, reverse: 5′-GGCTAC AGGCTTGTCACTCGG-3′). An 1 μL portion of the reverse-transcribed mixture was added to a PCR mixture containing 10 pmol of each primer and 10 μL of SYBR Premix ExTaq solution in a final volume of 20 μL. After an initial denaturation at 95°C for 30 s, the amplification was performed by denaturation at 94°C for 20 s and annealing and extension at 64°C for 20 s for 45 cycles. The IL-8 and TNFα mRNA levels were normalized with human glyceraldehyde 3-phosphate dehydrogenase (GAPDH) mRNA (forward: 5′-CCATGAGAAGTATGACAACAGCC-3′, 5′-TG GGTGGCAGTGATGGCATGGA-3′).

Immunoblot analysis

SDS–polyacrylamide gel electrophoresis and immunoblot analysis were performed according to Laemmli (1970). Cell sources (25 μg) were separated on 10% polyacrylamide gels and electrotransferred onto polyvinylidene difluoride membrane, Immobilon-P (Millipore Corporation, Billerica, MA). The membranes were probed with the monoclonal antibodies of anti-Thr202/Tyr204 phosphorylated ERK1/2, anti-Thr180/Tyr182 phosphorylated p38 MAP kinase, and anti-Thr183/Tyr185 phosphorylated JNK1/2, and the corresponding fluorescent dye-conjugated second antibody and an Odyssey Infrared Imaging system (LI-COR Biosciences, Lincoln, NE) were used for the detection. The relative expression level was quantified using ImageQuant TL Image Analysis software (GE Healthcare, Little Chalfont, Buckinghamshire, UK).

Cell viability assay

For the cell viability assay, THP-1 cells were seeded at a density of 1×10^5 cells/well in 96-well plates with the medium containing the indicated concentration of the halminthic drug, and then incubated at 37°C. The final concentration of DMSO in medium was 0.1%. After 6 or 24 h incubation, cell viability was evaluated by 3-(4,5-dimetylthiazol-2-yl)-2, 5-diphenyl tetrazolium bromide (MTT) activities using a CellTiter-Blue Cell Viability Assay (Promega, Medison, WI) according to the manufacturer's protocol. The fluorescence of the generated resorufin was detected fluorometrically (excitation: 338 nm, emission: 458 nm) by using a luminometer (1420 ARVO MX, Wallac, Turku, Finland).

Statistical analysis

Data are expressed as mean ± SD of triplicate determinations. Comparison of 2 groups was made with an unpaired, two-tailed student's *t*-test. Comparison of multiple groups was made with ANOVA followed by Dunnett or Tukey test. A value of $P < 0.05$ was considered statistically significant.

Results

Comparative effect of helminthic drugs on human monocytic cell lines

To investigate whether the helminthic drugs increased the release of IL-8 and TNFα from human monocytic cells, cells were treated with 10 μM of the helminthic drugs for 6 h and then the release of IL-8 and TNFα in the cell supernatants was measured by ELISA. The helminthic drugs used in our study are shown in Fig. 1. ABZSO was the active metabolite of ABZ (Gottschall et al. 1990). FBZ and OBZ were used as drugs structurally similar to MBZ and ABZ, although they have never been administered in humans. PZQ was used because no case of symptomatic hepatic injury has ever been seen so far. The IL-8 and TNFα release from THP-1 cells was significantly increased by treatment with ABZ, FBZ, MBZ, or OBZ but not by ABZSO or PZQ compared with control (0.1% DMSO) (Fig. 2a, b). These results suggested that MBZ and structurally similar drugs have the ability to increase the release of pro-inflammatory cytokines and chemokines from monocytes that activate the inflammatory responses. In addition, MBZ and OBZ also significantly increased the IL-8 release from HL-60 and KG-1 cells and FBZ significantly increased the IL-8 release from KG-1 cells (Fig. 2c, e). In contrast, the TNFα release from HL-60 and KG-1 cells was not increased by these helminthic drugs (Fig. 2d, f). For the subsequent analyses, THP-1 cells were used because they showed the highest sensitivity for the release.

Time-dependent changes in the mRNA expression levels and the release of IL-8 and TNFα in THP-1 cells treated with MBZ

We next investigated the time-dependent changes of the IL-8 and TNFα levels in THP-1 cells. By the treatment

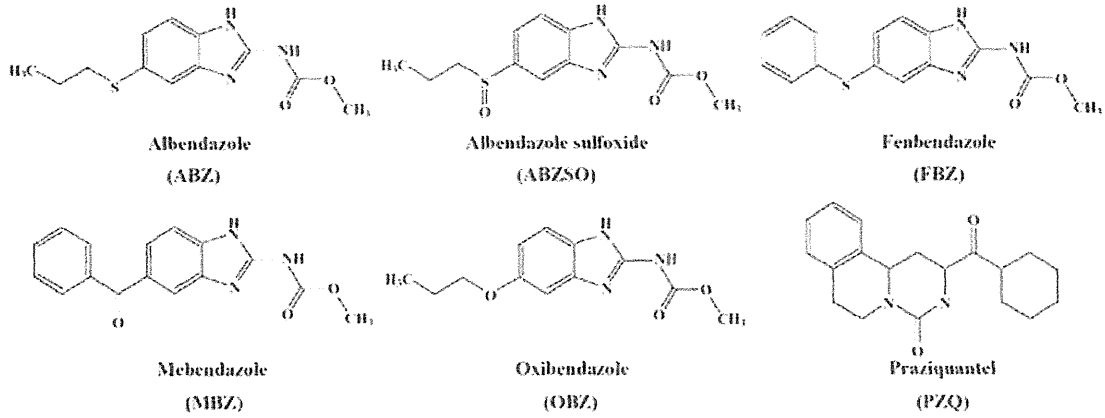

Fig. 1 Chemical structures of the helminthic drugs used in the present study

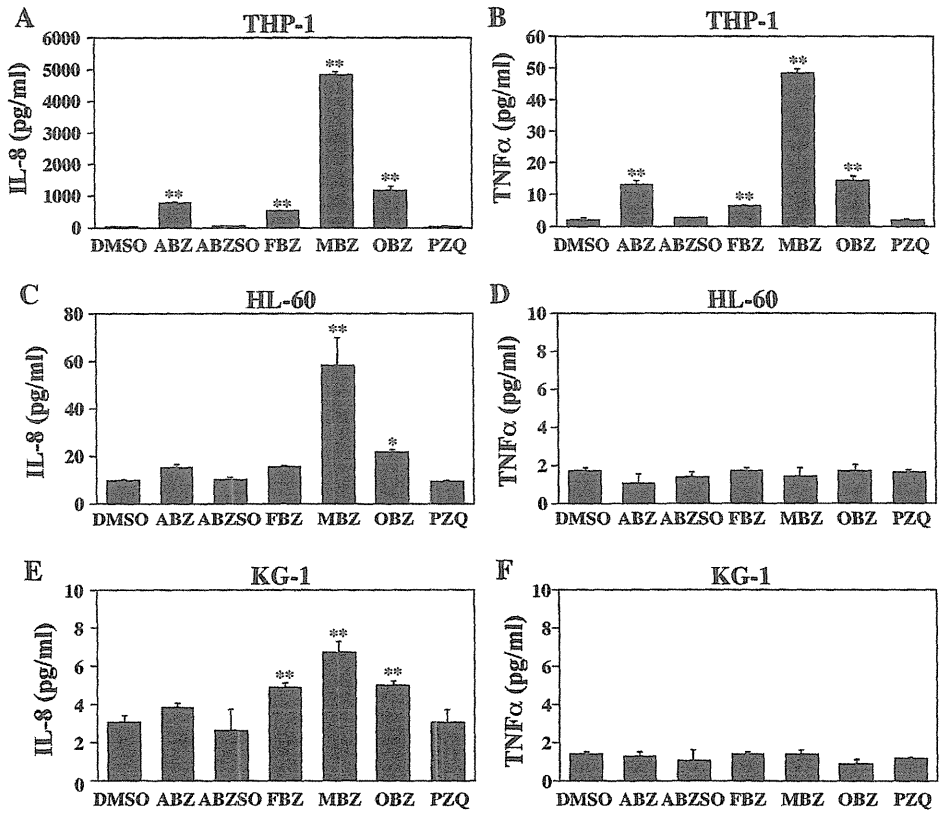

Fig. 2 Effects of helminthic drugs on the release of IL-8 and TNFα from human monocytic cell lines. Human monocytic cell lines including THP-1 (**a** and **b**), HL-60 (**c** and **d**), and KG-1 (**e** and **f**) were treated with 10 μM of the helminthic drugs for 6 h. The release of IL-8 (**a**, **c**, and **e**) and TNFα (**b**, **d**, and **f**) in the supernatant was measured by ELISA. Data represent the mean ± SD of triplicate determinations. $^{*}P < 0.05$; $^{**}P < 0.01$, compared with control (0.1% DMSO)

with 10 μM MBZ, the mRNA expression levels and the release of IL-8 and TNFα in THP-1 cells were significantly increased for 1.5–24 h compared with control (Fig. 3). The mRNA expression levels of IL-8 were mostly increased at 6 h incubation but the increase of IL-8 release was in a time-dependent manner (Fig. 3a, c). The highest increase of the mRNA expression levels and the release of TNFα appeared at 4.5 and 6 h-incubation, respectively (Fig. 3b, d). Therefore, an incubation time of 6 h was selected for further assay to measure the release of IL-8 and TNFα. To investigate whether there were cytotoxic effects on THP-1 cells caused by the leakage of intercellular cytokines and chemokines, a cell viability assay for THP-1 cells was performed. At 24 h-incubation, these helminthic drugs had no cytotoxic effects on THP-1 cells (data not shown).

Dose-dependent changes in the release of IL-8 and TNFα from THP-1 cells treated with helminthic drugs

To investigate whether the helminthic drugs at a lower concentration could also lead to IL-8 and TNFα release in

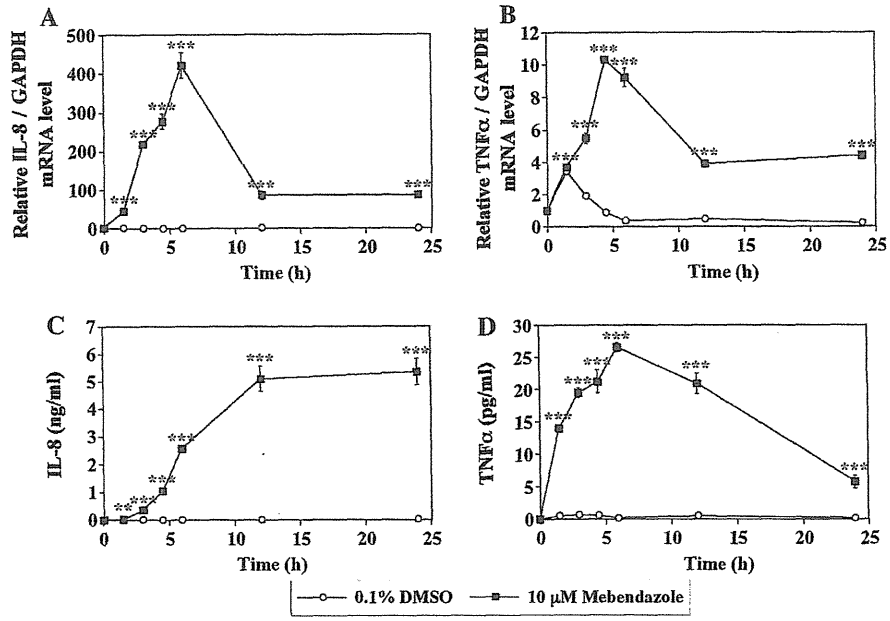

Fig. 3 Time-dependent changes in the mRNA expression levels and the release of IL-8 and TNFα in THP-1 cells treated with MBZ. THP-1 cells were treated with 10 μM MBZ for various durations. The mRNA expression levels of IL-8 (**a**) and TNFα (**b**) in THP-1 cells were measured by real-time RT–PCR analysis. The release of IL-8 (**c**) and TNFα (**d**) in the supernatant was measured by ELISA. Data represent the mean ± SD of triplicate determinations. $^{**}P < 0.01$; $^{***}P < 0.001$, compared with control (0.1% DMSO) of each time point

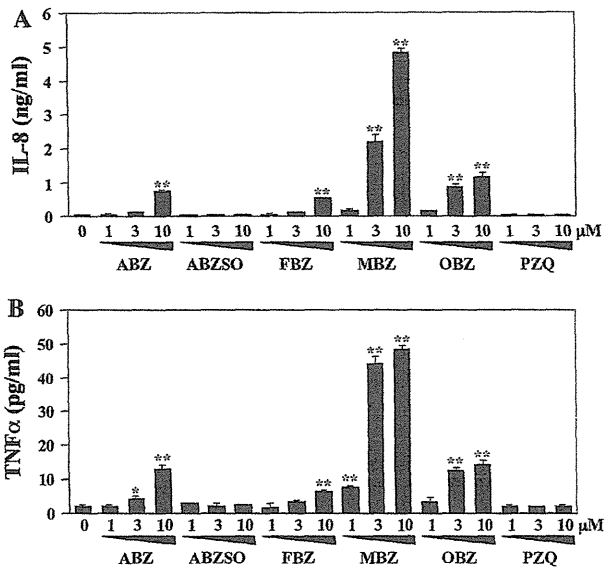

Fig. 4 Dose-dependent changes in the release of IL-8 and TNFα from THP-1 cells treated with helminthic drugs. THP-1 cells were treated with the indicated concentrations of the helminthic drugs. After incubation for 6 h, the release of IL-8 (**a**) and TNFα (**b**) in the supernatant was measured by ELISA. Data represent the mean ± SD of triplicate determinations. $^{*}P < 0.05$; $^{**}P < 0.01$, compared with control (0.1% DMSO)

THP-1 cells, THP-1 cells were treated with helminthic drugs at the indicated concentration for 6 h and then the release of IL-8 and TNFα was measured. As shown in Fig. 4, ABZ, FBZ, MBZ, and OBZ increased the IL-8 and TNFα levels in a dose-dependent manner. In addition, at least 3 μM MBZ was required to increase the release of IL-8 in THP-1 cells. In contrast, the TNFα release was significantly increased at 1 μM MBZ.

Activation of MAP kinase signaling pathway in THP-1 cells treated with MBZ

MAP kinases, including ERK1/2, p38 MAP kinase, and JNK1/2, are major components for many intracellular signaling pathways. The phosphorylation of MAP kinases, which is required for the enzyme activity, activates signaling cascades, the down stream effects of which have been linked to the regulation of the inflammatory response (DeFranco et al. 1998). To clarify the role of MAP kinase signaling pathway in the activation of THP-1 cells, the phosphorylation of ERK1/2 (44/42 kDa), p38 MAP kinase (43 kDa), and JNK1/2 (46/54 kDa) in cell lysates was assessed by immunoblot analysis. A sample treated with 2 μg/ml LPS was used as a positive control for the phosphorylation of MAP kinases. As shown in Fig. 5, MBZ treatment for 1 h significantly increased the phosphorylation of ERK1/2 and JNK1/2 but not p38 MAP kinase in THP-1 cells. These results suggested that MBZ activated ERK1/2 and JNK1/2 pathways in THP-1 cells. In addition, to confirm the effects of MAP kinase inhibitors on the phosphorylation of ERK1/2, p38 MAP kinase, and JNK1/2, THP-1 cells were pretreated for 1 h with various concentrations of MEK1/2 inhibitor U0126, p38 MAP kinase inhibitor SB203580, or JNK1/2 inhibitor SP600125 (English and Cobb, 2002) before the treatment with 10 μM MBZ. As a result, the phosphorylation of ERK1/2 was significantly suppressed by the pretreatment with the specific inhibitor U0126 but not that of JNK1/2 (Fig. 5).

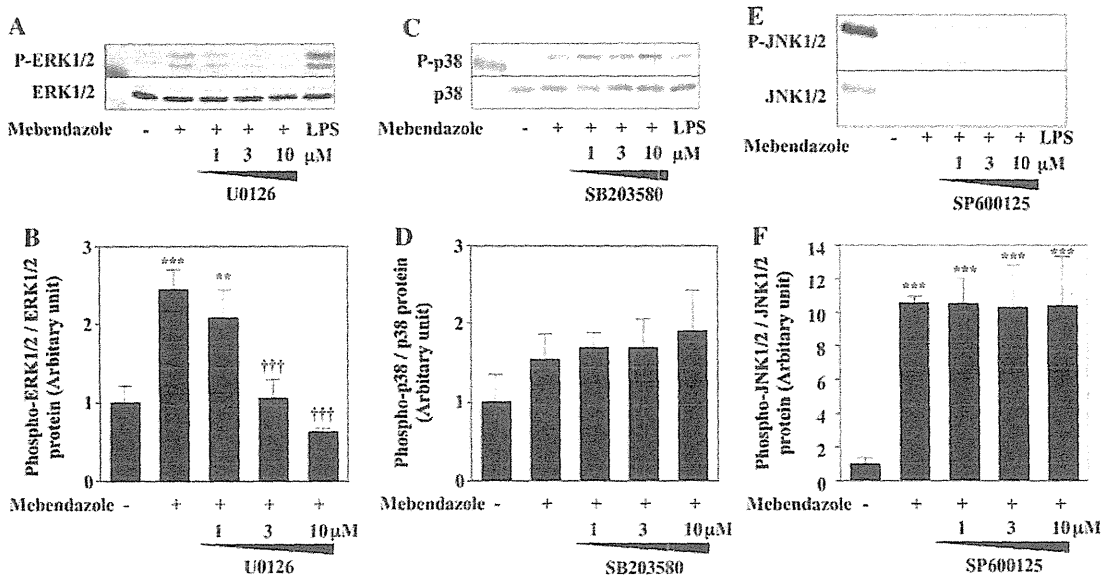

Fig. 5 Activation of MAP kinase signaling pathways in THP-1 cells treated with MBZ. Immunoblot analyses of MAP kinase proteins in THP-1 cells were performed (**a**, **c**, and **e**) and quantified (**b**, **d**, and **f**). Before the treatment with 10 μM MBZ, THP-1 cells were pretreated with the indicated concentrations of MAP kinase inhibitors for 1 h. U0126, SB203580, and, SP600125 were used as specific inhibitors of MEK1/2, p38 MAP kinase, and, JNK1/2, respectively. After 1 h-incubation with MBZ, cell lysates were subjected to immunoblot analyses using antibodies of anti-Thr202/Tyr204 phosphorylated ERK1/2 (**a** and **b**), anti-Thr180/Tyr182 phosphorylated p38 MAP kinase (**c** and **d**), and anti-Thr183/Tyr185 phosphorylated JNK1/2 (**e** and **f**). The same sample treated with 2 μg/ml LPS was used as a positive control. Data represent the mean ± SD of triplicate determinations. $^{**}P < 0.01$; $^{***}P < 0.001$, compared with control (0.1% DMSO). $\dagger\dagger P < 0.01$; $\dagger\dagger\dagger P < 0.001$, compared with MBZ only

The phosphorylation of JNK1/2 treated with LPS was suppressed by the pretreatment with the specific inhibitor SP600125 (data not shown).

Effects of MAP kinase inhibitors on the release of IL-8 and TNFα from THP-1 cells treated with helminthic drugs

To clarify which MAP kinase signaling pathway is mainly involved in the increase of IL-8 and TNFα release, the effects of MAP kinase inhibitors on the release of IL-8 and TNFα from THP-1 cells treated with MBZ were investigated. As shown in Fig. 6, the increased release of IL-8 and TNFα by MBZ treatment from THP-1 cells was significantly suppressed in a dose dependent manner by the pretreatment with U0126, suggesting that an ERK1/2 pathway plays an important role in the release of IL-8 and TNFα by MBZ treatment. A suppressing effect by SP600125 was not observed. In contrast, the increase of IL-8 and TNFα release was enhanced by the pretreatment with SB203580. Therefore, we investigated the effects of MAP kinase inhibitors on the release of IL-8 and TNFα from THP-1 cells treated with other helminthic drugs. As shown in Fig. 7, with ABZ, FBZ, or OBZ treatment, the pretreatment with U0126 remarkably suppressed the increase of IL-8 and TNFα in THP-1 cells and those of SB203580 and SP600125 had no suppressive effects. These results suggested that an ERK1/2 pathway also plays an important role in the increase of IL-8 and TNFα by ABZ, FBZ, or OBZ treatment as well as MBZ treatment. In contrast, even for the control, the basal IL-8 and TNFα levels in THP-1 cells were significantly suppressed by the pretreatment with U0126 and were increased by the pretreatment with SB203580, suggesting that the basal IL-8 and TNFα levels in THP-1 cells were affected by the MAP kinase inhibitors. In the case of ABZSO and PZQ, the effects of MAP kinase inhibitors on the IL-8 and TNFα levels in THP-1 cells were similar to those of the control (0.1% DMSO).

Discussion

For in vitro studies of the differentiation and activation of immune cells, human monocytic cell lines, THP-1, HL-60, and KG-1 cells are usually employed. In the present study, by the treatment with the helminthic drugs MBZ, IL-8 release from THP-1, HL-60, and KG-1 cells and TNFα release from THP-1 cells was significantly increased compared with the control (Fig. 2a–c, e). In the case of ABZ, FBZ, or OBZ, the release of IL-8 and TNFα from THP-1 cells was also significantly increased compared with the control (Fig. 2a, b). This suggested that MBZ and structurally similar drugs have the ability to stimulate the

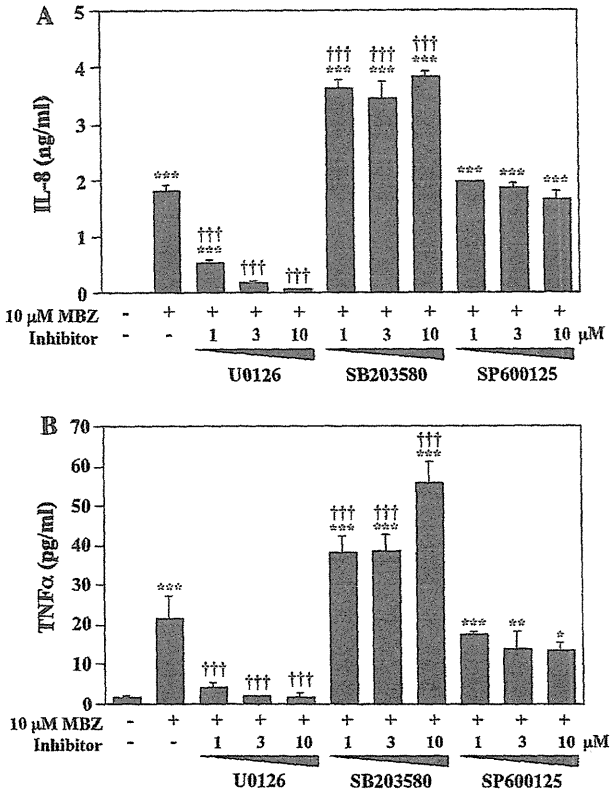

Fig. 6 Effects of MAP kinase inhibitors on the IL-8 and TNFα release from THP-1 cells treated with MBZ. Before the treatment with 10 μM MBZ, THP-1 cells were pretreated with the indicated concentrations of MAP kinase inhibitors for 1 h. After 6 h-incubation with MBZ, the release of IL-8 (**a**) and TNFα (**b**) in the supernatant was measured by ELISA. Data represent the mean ± SD of triplicate determinations. $^{*}P < 0.05$; $^{**}P < 0.01$; $^{***}P < 0.001$, compared with control (0.1% DMSO). $\dagger P < 0.05$; $\dagger\dagger P < 0.01$; $\dagger\dagger\dagger P < 0.001$, compared with MBZ only

release of pro-inflammatory cytokines from monocytes, leading to the activation of the inflammatory reaction. In contrast, PZQ, used as a negative control for MBZ, had no effects on the cytokine release in human monocytic cells. This result was supported by the fact that no case of symptomatic hepatic injury has ever been seen so far.

We found that MBZ stimulates the release of pro-inflammatory cytokines and chemokines from human monocytic cells. The activation of inflammatory responses might be one of the mechanisms underlying the immune-mediated liver injury by MBZ. On the other hand, the activation of human monocytic cells by other drugs, such as ximelagatran and troglitazone, has been reported recently, although these drugs have already been withdrawn from the market due to idiosyncratic hepatic injury (Edling et al. 2008, 2009). Ximelagatran increased the release of chemokines from THP-1 cells but the types of released cytokines and the time dependent change of the cytokine release by the drug treatment were different from the case of MBZ (Edling et al. 2008). In addition, troglitazone increased the mRNA expression levels of pro-inflammatory cytokines and chemokines in THP-1 cells (Edling et al. 2009). Therefore, measurement of the release of pro-inflammatory cytokines and chemokines from human monocytic cells may be useful to predict the possibility of adverse reactions to drugs involving immune-mediated hepatic injury.

The activation of MAP kinases such as ERK1/2, p38 MAP kinase, and JNK1/2 is important in mediating many macrophage functions, including the activation of various transcription factors and the production of pro-inflammatory cytokines (Payne et al. 1991; DeFranco et al.

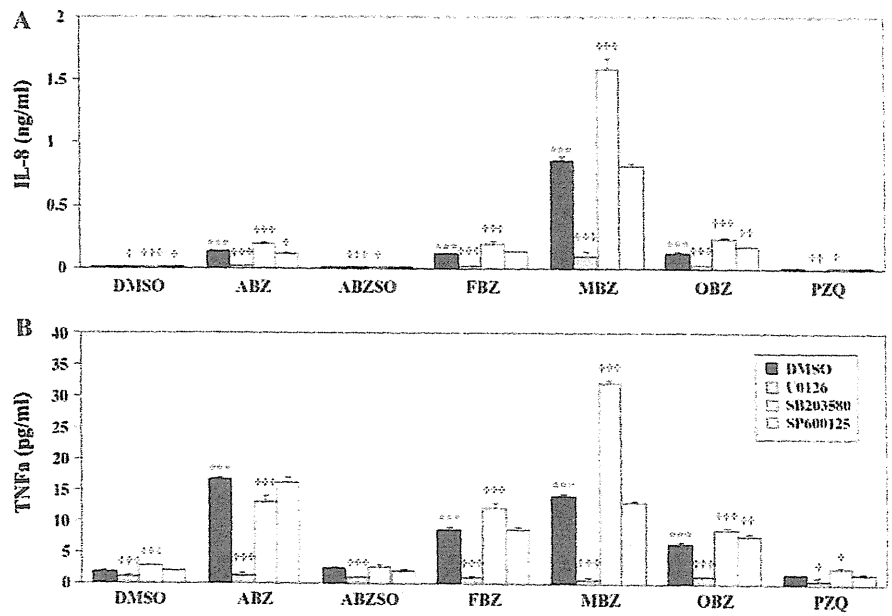

Fig. 7 Effects of MAP kinase inhibitors on the IL-8 and TNFα release from THP-1 cells treated with helminthic drugs. Before the incubation with 10 μM of the helminthic drugs, THP-1 cells were pretreated with 10 μM MAP kinase inhibitors for 1 h. After 6 h-incubation with the halminthic drugs, the release of IL-8 (**a**) and TNFα (**b**) in the supernatant was measured by ELISA. Data represent the mean ± SD of triplicate determinations. $^{***}P < 0.001$, compared with control (0.1% DMSO). $\dagger P < 0.05$; $\dagger\dagger P < 0.01$; $\dagger\dagger\dagger P < 0.001$, compared with an helminthic drug only

1998). In this study, MBZ activated the ERK1/2 and JNK1/2 pathways in THP-1 cells (Fig. 6). Previous experiments with several MAP kinase inhibitors demonstrated that blocking MAP kinase prevents IL-8 and TNFα release from LPS-stimulated monocytes at the transcription and translation levels (Guha and Mackman 2001). To determine the involvement of MAP kinases in MBZ-induced IL-8 and TNFα release, blocking studies were performed using specific inhibitors of MAP kinases, including U0126, SB203580, and SP600125 (English and Cobb 2002). The release of IL-8 and TNFα increased by MBZ was significantly suppressed by the U0126 pretreatment (Figs. 5, 6). These results suggested that an ERK pathway is mainly involved in IL-8 and TNFα release from THP-1 cells. In addition, the increase of IL-8 and TNFα release from THP-1 cells was enhanced by the pretreatment with SB203580 (Fig. 5). At higher concentrations, the p38 MAP kinase inhibitors have been reported to increase the phosphorylation of ERK1/2 (Ishii et al. 2001; Hirosawa et al. 2009). THP-1 cells also have been reported to show enhanced ERK cascade by SB203580 (Numazawa et al. 2003). Considering these reports, the increase of IL-8 and TNFα release from THP-1 cells by SB203580 would be due to the activation of an ERK pathway.

Elevations of serum aminotransferases have been reported to occur in 9–13% of patients treated with 50–100 mg/kg/day; however, severe hepatic injury of MBZ is very rare. Seitz et al. (1983) and Junge and Mohr (1983) reported MBZ-induced hepatic injury, and liver biopsy of the patient revealed hepatocytic necrosis and portal inflammation with eosinophils during long-term (49–60 days) and high-dose (2–3.5 g/day) therapy with MBZ. Rechallenge was followed by a marked elevation of the aminotranferase levels. Liver biopsy showed hepatocytic necrosis and portal inflammation with eosinophils (Junge and Mohr 1983), suggesting an immune-mediated drug response. Colle et al. (1999) also reported a case of granulomatous (immunoallergic) hepatitis with eosinophilia after the administration of MBZ.

It has been reported that the peak plasma concentrations of MBZ was 0.12 ± 0.08 μM 2 h after a single oral administration of 1000 mg MBZ in 16 healthy volunteers (Corti et al. 2009). Because it is very difficult to predict actual drug concentration in the liver and to extrapolate from an in vitro study to the in vivo condition in humans, it is better to test the drug effects in cell-based assays at a range of concentrations up to at least 30 times the efficacious concentration as reported by O'Brien et al. (2006). Thus, we conducted with up to 10 μM of MBZ. However, further study is necessary to clarify whether oral administration of MBZ stimulates the release of pro-inflammatory cytokines and chemokines in vivo.

We obtained ABZSO, an active metabolite of ABZ, which was investigated in this study as a structurally similar drug. ABZSO would be responsible for the systemic biological activity of ABZ, whereas ABZ sulfone is pharmacologically inert (Gottschall et al. 1990). A case report of acute hepatitis caused by ABZ was recently reported by Choi et al. (2008). In evaluating the relation of ABZ and ABZSO to the cytokine release, interestingly, pro-inflammatory cytokine release was found to be increased by treatment with ABZ, but not by ABZSO treatment in human monocytic cells (Figs. 2, 7). These results suggested that ABZ is a causal drug of hepatic injury. However, the activation of THP-1 cells by MBZ was much higher than that by ABZ.

In conclusion, we found that MBZ stimulated human monocytic THP-1 cells resulting in IL-8 and TNFα release. It is suggested that MBZ increases the pro-inflammatory cytokine release from monocytes and macrophages and activates the inflammatory response, which might result in immune-mediated hepatic injury. The findings presented here provide important insight concerning MBZ-induced liver injury.

Acknowledgments We thank Mr. Brent Bell for reviewing the manuscript. This work was supported by Health and Labor Sciences Research Grants from the Ministry of Health, Labor, and Welfare of Japan (H20-BIO-G001).

References

Ammann RW, Eckert J (1996) Cestodes. Echinococcus. Gastroenterol Clin North Am 25:655–689

Baggiolini M, Dewald B, Moser B (1994) Interleukin-8 and related chemotactic cytokines-CXC and CC chemokines. Adv Immunol 55:97–179

Bagheri H, Simiand E, Montastruc JL, Magnaval JF (2004) Adverse drug reactions to anthelmintics. Ann Pharmacother 38:383–388

Bekhti A, Pirotte J (1987) Hepatotoxicity of mebendazole, Relationship with serum concentrations of the drug. Gastroenterol Clin Biol 11:701–703

Bradham CA, Plümpe J, Manns MP, Brenner DA, Trautwein C (1998) Mechanisms of hepatic toxicity. I. TNF-induced liver injury. Am J Physiol 275:G387–G392

Chen K-T, Twu S-J, Chen H-J, Lin R-S (2003) Outbreak of Steravens-Johnson syndrome/toxic epidermal necrolysis associated with mebendazole and metronidazole use among Filipino laborers in Taiwan. Am J Public Health 93:489–492

Choi GY, Yang HW, Cho SH, Kang DW, Go H, Lee WC, Lee YJ, Jung SH, Kim AN, Cha SW (2008) Acute drug-induced hepatitis caused by albendazole. J Korean Med Sci 23:903–905. doi: 10.3346/jkms.2008.23.5.903

Colle I, Naegels S, Hoorens A, Hautekeete M (1999) Granulomatous hepatitis due to mebendazole. J Clin Gastroenterol 28:44–45

Corti N, Heck A, Rentsch K, Zingg W, Jetter A, Stieger B, Pauli-Magnus C (2009) Effect of ritonavir on the pharmacokinetics of the benzimidazoles albendazole and mebendazole: an interaction study in healthy volunteers. Eur J Clin Pharmacol 65:999–1006

DeFranco AL, Crowley MT, Finn A, Hambleton J, Weinstein SL (1998) The role of tyrosine kinases and map kinases in LPS-induced signaling. Prog Clin Biol Res 397:119–136

Deng X, Luyendyk JP, Ganey PE, Roth RA (2009) Inflammatory stress and idiosyncratic hepatotoxicity: hints from animal models. Pharmacol Rev 61:262–282. doi:10.1124/pr.109.001727

Edling Y, Sivertsson L, Andersson TB, Porsmyr-Palmertz M, Ingelman-Sundberg M (2008) Pro-inflammatory response and adverse drug reactions: mechanisms of action of ximelagatran on chemokine and cytokine activation in a monocyte in vitro model. Toxicol In Vitro 22:1588–1594. doi:10.1016/j.tiv.2008.06.011

Edling Y, Sivertsson LK, Butura A, Ingelman-Sundberg M, Ek M (2009) Increased sensitivity for troglitazone-induced cytotoxicity using a human in vitro co-culture model. Toxicol In Vitro 23:1387–1395. doi:10.1016/j.tiv.2009.07.026

English JM, Cobb MH (2002) Pharmacological inhibitors of MAPK pathways. Trends Pharmacol Sci 23:40–45

Ganey PE, Luyendyk JP, Maddox JF, Roth RA (2004) Adverse hepatic drug reactions: inflammatory episodes as consequence and contributor. Chem Biol Interact 150:35–51. doi:10.1016/j.cbi.2004.09.002

Gottschall DW, Theodorides VJ, Wang R (1990) The metabolism of benzimidazole anthelmintics. Parasitol Today 6:115–124

Guha M, Mackman N (2001) LPS induction of gene expression in human monocytes. Cell Signal 13:85–94

Hirosawa M, Nakahara M, Otosaka R, Imoto A, Okazaki T, Takahashi S (2009) The p38 pathway inhibitor SB202190 activates MEK/MAPK to stimulate the growth of leukemia cells. Leuk Res 33:693–699. doi:10.1016/j.leukres.2008.09.028

Holt MP, Ju C (2006) Mechanisms of drug-induced liver injury. AAPS J 8:E48–E54. doi:10.1208/aapsj080106

Ishii Y, Sakai S, Honma Y (2001) Pyridinyl imidazole inhibitor SB203580 activates p44/42 mitogen-activated protein kinase and induces the differentiation of human myeloid leukemia cells. Leuk Res 25:813–820

Jaeschke H (2005) Role of inflammation in the mechanism of acetaminophen-induced hepatotoxicity. Expert Opin Drug Metab Toxicol 1:389–397. doi:10.1517/17425255.1.3.389

Junge U, Mohr W (1983) Mebendazole-hepatitis. Z Gastroenterol 21:736–738

Laemmli UK (1970) Cleavage of structural proteins during the assembly of the head of bacteriophage T4. Nature 227:680–685

Leonard EJ, Yoshimura T, Tanaka S, Raffeld M (1991) Neutrophil recruitment by intradermally injected neutrophil attractant/activation protein-1. J Invest Dermatol 96:690–694

Numazawa S, Watabe M, Nishimura S, Kurosawa M, Izuno M, Yoshida T (2003) Regulation of ERK-mediated signal transduction by p38 MAP kinase in human monocytic THP-1 cells. J Biochem 133:599–605

O'Brien PJ, Irwin W, Diaz D, Howard-Cofield E, Krejsa CM, Slaughter MR, Gao B, Kaludercic N, Angeline A, Bernardi P, Brain P, Hougham C (2006) High concordance of drug-induced human hepatotoxicity with in vitro cytotoxicity measured in a novel cell-based model using high content screening. Arch Toxicol 80:580–604

Payne DM, Rossomando AJ, Martino P, Erickson AK, Her JH, Shabanowitz J, Hunt DF, Weber MJ, Sturgill TW (1991) Identification of the regulatory phosphorylation sites in pp42/mitogen-activated protein kinase (MAP kinase). EMBO J 10:885–892

Roth RA, Luyendyk JP, Maddox JF, Ganey PE (2003) Inflammation and drug idiosyncrasy-is there a connection? J Pharmacol Exp Ther 307:1–8. doi:10.1124/jpet.102.041624

Seitz R, Schwerk W, Arnold R (1983) Hepatocellular drug reactions caused by mebendazole therapy in cystic echinococcosis. Z Gastroenterol 21:324–329

Tafazoli S, Spehar DD, O'Brien PJ (2005) Oxidative stress mediated idiosyncratic drug toxicity. Drug Metab Rev 37:311–325. doi:10.1081/DMR-55227

0090-9556/11/3901-54–60$20.00
DRUG METABOLISM AND DISPOSITION
Copyright © 2011 by The American Society for Pharmacology and Experimental Therapeutics
DMD 39:54–60, 2011

Vol. 39, No. 1
35600/3650890
Printed in U.S.A.

Toxicological Evaluation of Acyl Glucuronides of Nonsteroidal Anti-Inflammatory Drugs Using Human Embryonic Kidney 293 Cells Stably Expressing Human UDP-Glucuronosyltransferase and Human Hepatocytes[S]

Toshihisa Koga, Ryoichi Fujiwara, Miki Nakajima, and Tsuyoshi Yokoi

Drug Metabolism and Toxicology, Faculty of Pharmaceutical Sciences, Kanazawa University, Kanazawa, Japan

Received July 23, 2010; accepted October 6, 2010

ABSTRACT:

The chemical reactivity of acyl glucuronide (AG) has been thought to be associated with the toxic properties of drugs containing carboxylic acid moieties, but there has been no direct evidence that AG formation was related to the toxicity. In the present study, the cytotoxicity and genotoxicity of AGs were investigated. Human embryonic kidney (HEK) 293 cells stably expressing UDP-glucuronosyltransferase (UGT) 1A3 (HEK/UGT1A3) were constructed to assess the cytotoxicity of AGs, and HEK/UGT1A4 cells were also used as a negative reference. After exposure to nonsteroidal anti-inflammatory drugs (NSAIDs) such as naproxen (1 mM), diclofenac (0.1 mM), ketoprofen (1 mM), or ibuprofen (1 mM) for 24 h, HEK/UGT1A3 cells produced AG in a time-dependent manner. However, HEK/UGT1A4 cells hardly produced AG. The cytotoxicity of HEK/UGT1A3 cells was not increased compared with that of HEK/UGT1A4 cells. In addition, the AG formed in NSAID-treated human hepatocytes was decreased from one-third to one-ninth by treatment with (−)-borneol, an inhibitor of acyl glucuronidation, but the cytotoxicity was increased. These results indicated that AG formation reflected the detoxification process in human hepatocytes. Furthermore, the possibility of genotoxicity from the AG formed in NSAID-treated HEK/UGT cells was investigated by the comet assay, and DNA damage was not detected in any HEK/UGT cell lines. In conclusion, the in vitro cytotoxic and genotoxic effects of the AGs of NSAIDs were investigated and AG was not found to be a causal factor in the toxicity.

Introduction

Some of the most commonly prescribed medications and over-the-counter drugs are carboxylate compounds, including many nonsteroidal anti-inflammatory drugs (NSAIDs) and fibrate lipid-lowering drugs. Approximately 25% of drugs withdrawn from the market around the world because of severe toxicity have been carboxylic acids, such as the NSAIDs ibufenac, zomepirac, bromfenac, suprofen, and benoxaprofen. Among drugs containing carboxylic acid, NSAIDs are associated with some degree of hepatotoxicity, immune cytopenias, and hypersensitivity reactions (Bailey and Dickinson, 2003). However, the essential cause of the toxicity is uncertain because of the structural diversity of NSAIDs. For example, diclofenac is associated with hepatotoxicity with a low incidence of 6 to 18 cases/100,000 person-years (Walker, 1997). Both immunological and nonimmunological mechanisms have been proposed to be responsible for the diclofenac hepatotoxicity (Banks et al., 1995; Wade et al., 1997).

Glucuronidation is one of the most important phase II metabolic pathways for endogenous and exogenous substrates in humans. Because glucuronides usually possess less intrinsic biological or chemical activity than their parent aglycones and are rapidly excreted, glucuronidation is considered to be a detoxification reaction (Shipkova et al., 2003). However, acyl glucuronide (AG), which is characterized by its electrophilic reactivity, has been implicated in a wide range of adverse drug effects including drug hypersensitivity reactions and cellular toxicity (Ritter, 2000). It is well known that AG is unstable in physiological conditions and consequently undergoes hydrolysis or intramolecular rearrangement, which occurs by migration of the drug moiety from the 1-*O*-β position to 2-, 3-, and 4-positions on the glucuronic acid ring (Bailey and Dickinson, 2003; Shipkova et al., 2003). As a result, AG potentially binds to cellular macromolecules covalently and has been suspected to mediate idiosyncratic drug toxicities associated with carboxylic drugs (Boelsterli et al., 1995).

This study was supported by the Ministry of Health, Labor, and Welfare of Japan [Health and Labor Sciences Research Grant H20-B10-G001].

Article, publication date, and citation information can be found at http://dmd.aspetjournals.org.

doi:10.1124/dmd.110.035600.

[S] The online version of this article (available at http://dmd.aspetjournals.org) contains supplemental material.

ABBREVIATIONS: NSAID, nonsteroidal anti-inflammatory drug; AG, acyl glucuronide; UGT, UDP-glucuronosyltransferase; HEK, human embryonic kidney; DMSO, dimethyl sulfoxide; UDPGA, UDP-glucuronic acid; 4-MU, 4-methylumbelliferone; GAPDH, glyceraldehyde-3-phosphate dehydrogenase; PAGE, polyacrylamide gel electrophoresis; PBS, phosphate-buffered saline; HPLC, high-performance liquid chromatography; FBS, fetal bovine serum; DMEM, Dulbecco's modified Eagle's medium; LC, liquid chromatography; MS/MS, tandem mass spectrometry; MTT, 3-(4,5-dimethylthiazol-2-yl)-2,5-diphenyltetrazolium; WST-8, 2-(2-methoxy-4-nitrophenyl)-3-(4-nitrophenyl)-5-(2, 4-disulfophenyl)-2*H*-tetrazolium monosodium salt; LDH, lactic dehydrogenase.

Until now, both direct toxic effects and immune-mediated toxicity have been suggested as possible mechanisms of idiosyncratic liver injury. With direct toxicity, covalent protein binding via AG may disrupt the normal physiological function of a "critical" protein or some critical regulatory pathway, leading to cellular necrosis (Pirmohamed et al., 1996). In addition, it has been reported that electrophilic AG can covalently interact with nucleic acids. For example, clofibrate AG and gemfibrozil AG can form DNA adducts, resulting in genotoxicity that can be measured by the single-cell gel electrophoresis (comet) assay (Sallustio et al., 1997). Furthermore, probenecid and clofibric acid induced DNA damage in isolated hepatocytes and UDP-glucuronosyltransferase (UGT)-transfected HEK293 cells via a glucuronidation-dependent pathway (Sallustio et al., 2006; Southwood et al., 2007). The significance of these finding is not yet clear.

Among UGT isoforms, the glucuronidation of carboxylic acid drugs is mediated by UGT1A3, UGT1A9, or UGT2B7 (Sakaguchi et al., 2004). Of interest, despite high sequence identity (amino acid homology of 93%), human UGT1A3 and UGT1A4 differ in terms of substrate selectivity, i.e., UGT1A3 catalyzes the acyl glucuronidation but UGT1A4 hardly does (Kubota et al., 2007). HEK293 cells can express human recombinant UGTs for cytotoxicity studies and effectively glycosylate them (Nakajima et al., 2010; Nishiyama et al., 2010). Therefore, HEK293 cells stably expressing UGT1A3 (HEK/UGT1A3) and UGT1A4 (HEK/UGT1A4) could be useful for toxicity assessment.

Among the drugs containing the carboxylic acid moieties, naproxen, diclofenac, ketoprofen, and ibuprofen were selected. Naproxen, diclofenac, and ibuprofen infrequently show severe drug-induced liver injury, but ketoprofen almost never does (Cuthbert, 1974; Banks et al., 1995; Boelsterli et al., 1995; Walker, 1997; Riley and Smith, 1998). In addition, these NSAIDs are mainly metabolized to the corresponding AG (Foster et al., 1988; Vree et al., 1993; Castillo and Smith, 1995; Kumar et al., 2002). Direct mechanistic evidence linking the toxicity to the formation of drug-protein adducts is lacking. We focused on toxicity due to cell dysfunction by acyl glucuronide formation. In this study, to clarify whether formation of AG occurred in the cells, rather than exposure to hydrophilic AG from outside the cells, which shows toxicity due to cell dysfunction by the adduct formation in vitro, we investigated the cytotoxicity of the NSAIDs exposed to HEK/UGT1A3 or HEK/UGT1A4 and human hepatocytes. Furthermore, we investigated the genotoxicity of the NSAIDs by using the comet assay.

Materials and Methods

Materials. Ketoprofen, ibuprofen, G418, and dimethyl sulfoxide (DMSO) were purchased from Wako Pure Chemicals (Osaka, Japan). Naproxen acyl-β-D-glucuronide, diclofenac acyl-β-D-glucuronide, ketoprofen acyl-β-D-glucuronide, and ibuprofen acyl-β-D-glucuronide were purchased from Toronto Research Chemicals Inc. (North York, ON, Canada). Naproxen, diclofenac sodium salt, UDP-glucuronic acid (UDPGA), alamethicin, 4-methylumbelliferone (4-MU), 4-MU *O*-glucuronide, and (−)-borneol were purchased from Sigma-Aldrich (St. Louis, MO). Rabbit anti-human UGT1A antibodies were obtained from BD Gentest (Woburn, MA). Rabbit anti-human GAPDH antibodies were purchased from Imgenex (San Diego, CA). IRDye 680-labeled goat anti-rabbit secondary antibody and Odyssey Blocking buffer were obtained from LI-COR Biosciences (Lincoln, NE). Primers were commercially synthesized at Hokkaido System Sciences (Sapporo, Japan). Lipofectamine 2000 was purchased from Invitrogen (Carlsbad, CA). All other chemicals and solvents were of the highest grade or the analytical grade commercially available.

Isolation of Human UGT1A3 and Construction of Expression Vectors. Human UGT1A3 (accession number NM_019093) cDNAs were prepared by a reverse transcription-polymerase chain reaction technique using total RNA from human liver. The primer sequences used in this study were as follows: human UGT1A3ex1 sense primer, 5′-TCTTCTGCTGAGATGGCCAC-3′ and human UGT1Aex5 antisense primer, 5′-GCACTCTGGGGCTGATTAAT-3′. After an initial denaturation at 94°C for 5 min, amplification was performed by denaturation at 94°C for 30 s, annealing at 55°C for 30 s, and extension at 72°C for 90 s for 45 cycles, followed by a final extension at 72°C for 5 min. The polymerase chain reaction products were subcloned into pTARGET Mammalian Expression Vector (Promega, Madison, WI), and the DNA sequences of the inserts were determined using a Thermo Sequenase Cy5.5 Dye Terminator Cycle Sequencing Kit (GE Healthcare, Little Chalfont, Buckinghamshire, UK) with a Long-Read Tower DNA sequencer (GE Healthcare).

Stable Expression of UGT1A3 and UGT1A4 Isoforms in HEK293 Cells. An expression vector for UGT1A3 was constructed. HEK293 cells (American Type Culture Collection, Manassas, VA) were grown in Dulbecco's modified Eagle's medium containing 4.5 g/l glucose, 10 mM HEPES, and 10% fetal bovine serum with 5% CO_2 at 37°C. The cells in 12-well plates were transfected with 1.6 μg of the UGT1A3 expression vector using Lipofectamine 2000. Stable transfectants of UGT1A3 were selected in medium containing 800 mg/l G418. HEK293 cells stably expressing UGT1A4 were previously established in our laboratory (Fujiwara et al., 2007a). The cell lines were incubated with 95% O_2/5% CO_2 at 37°C and split 1:4 every 3 days.

SDS-PAGE and Immunoblotting. Samples were boiled for 3 min in Laemmli sample buffer containing 2-mercaptoethanol and separated on 10% SDS-polyacrylamide gel. The separated proteins were electrotransferred onto a polyvinylidene difluoride membrane (Immobilon-P; Millipore Corporation, Billerica, MA). The membrane was washed with phosphate-buffered saline (PBS) two times and blocked with Odyssey Blocking buffer for 1 h. The membranes were incubated with rabbit anti-human UGT1A polyclonal antibody (1:500) and rabbit anti-human GAPDH antibodies (1:1000) diluted with Odyssey Blocking buffer containing 0.1% Tween 20 for 1 h. The membrane was washed with PBS-T (PBS containing 0.1% Tween 20) four times and incubated with IRDye 680-labeled goat anti-rabbit IgG secondary antibody diluted (1:5000) with PBS-T for 1 h. The densities of the bands were determined using an Odyssey Infrared Imaging System (LI-COR Biosciences).

HPLC Analysis of 4-MU *O*-Glucuronide Formation on UGT1A3. 4-MU *O*-glucuronosyltransferase activity was determined as described previously with slight modifications (Fujiwara et al., 2007a). In brief, a typical incubation mixture (100 μl of total volume) contained 50 mM Tris-HCl buffer (pH 7.4), 10 mM $MgCl_2$, 2.5 mM UDPGA, 25 μg/ml alamethicin, 0.4 mg/ml cell homogenate of UGT1A3, and 1 to 1000 μM 4-MU. The reaction was initiated by the addition of UDPGA after a 3-min preincubation at 37°C. After incubation at 37°C for 30 min, the reaction was terminated by the addition of 100 μl of ice-cold methanol. After removal of the protein by centrifugation at 13,000*g* for 5 min, a 50-μl portion of the sample was subjected to HPLC. The analytical column was a CAPCEL PAK C18 UG120 (4.6 × 150 mm, 5 μm; Shiseido, Tokyo, Japan), and the mobile phase was 30% methanol-20 mM potassium phosphate buffer (pH 4.5). The eluent was monitored at 320 nm. The quantification of 4-MU *O*-glucuronide was performed by comparing the HPLC peak height with that of the authentic standard. Kinetic parameters were estimated from the fitted curve using a computer program (KaleidaGraph; Synergy Software, Reading, PA) designed for nonlinear regression analysis. The following equation was applied for Michaelis-Menten kinetics:

$$V = V_{max} \cdot S/(K_m + S)$$

where V is the velocity of the reaction, S is the substrate concentration, K_m is the Michaelis-Menten constant, and V_{max} is the maximum velocity. Data are expressed as means ± S.D. of triplicate determinations.

In Vitro Studies with HEK/UGT Cells. *Cytotoxicity assay.* HEK/UGT cells were seeded into 96-well microtiter plates layered with 2×10^4 cells/well in 0.1 ml of 0.5% (v/v) FBS supplemented DMEM and were immediately incubated with naproxen (1 mM), diclofenac (0.1 mM), ketoprofen (1 mM), or ibuprofen (1 mM) for 6, 12, or 24 h.

Quantification of the AG metabolites. HEK/UGT cells were seeded into 24-well plates layered with 2×10^5 cells/well in 1 ml of 0.5% (v/v) FBS-supplemented DMEM and were immediately incubated with the NSAIDs for 6, 12, or 24 h. The cultured cells were collected into a clean tube after the specified period and then centrifuged at 3000*g* for 5 min to separate the cultured medium and cell fraction. The cell fraction was suspended with 100 μl of PBS. We confirmed the stability of each AG in the autosampler at 4°C

for 24 h (data not shown). The final concentrations of DMSO in the culture medium did not exceed 0.1%.

In Vitro Studies with Human Hepatocytes. *Cytotoxicity assay.* LiverPool cryopreserved human hepatocytes in suspension (Celsis In Vitro Technologies, Brussels, Belgium) were seeded into collagen-coated 96-well microtiter plates layered with 2×10^4 cells/well in 0.1 ml of 0.5% (v/v) FBS-supplemented HCM culture medium (epidermal growth factor- and antibiotic-free) containing 10 nM estradiol and were immediately preincubated with (−)-borneol (1 mM), an inhibitor of acyl glucuronidation. After 30 min, the cells were incubated with the NSAIDs for 6 h.

Quantification of the NSAIDs and their AG metabolites. Human hepatocytes were seeded into collagen-coated 24-well plates layered with 2×10^5 cells/well in 1 ml of 0.5% (v/v) FBS-supplemented HCM culture medium and were immediately preincubated with (−)-borneol (1 mM). After 30 min, the cells were incubated with 0.5% (v/v) FBS-supplemented HCM culture medium containing the NSAIDs for 6 h. We confirmed the stability of each AG at 4°C for 24 h (data not shown). The final concentrations of DMSO in the culture medium did not exceed 0.2%.

LC-MS/MS Analysis and Preparation of AG Samples. The NSAIDs and their AGs were quantified using PE SCIEX API 2000 LC-MS/MS systems (MDS Sciex, Concord, ON, Canada) equipped with an electrospray ionization interface used to generate negative ions $[M - H]^-$. The test drugs were separated on a ZORBAX SB-C18 column (50 × 2.1 mm, 3.5 μm; Agilent Technologies, Santa Clara, CA). The gradient mobile phase consisted of 0.1% formic acid in purified water and 0.1% formic acid in methanol (80:20 to 10:90, v/v). The mobile phase was eluted at 0.2 ml/min using an Agilent 1100 series pump (Agilent Technologies). The NSAIDs and their AGs were monitored by multiple reaction monitoring using transitions of 229 → 169 (naproxen), 405 → 193 (naproxen AG), 294 → 250 (diclofenac), 470 → 193 (diclofenac AG), 253 → 209 (ketoprofen), 429 → 193 (ketoprofen AG), 205 → 161 (ibuprofen), and 381 → 193 (ibuprofen AG). These drugs were calculated by comparing the peak area to that of the authentic standard. The analytical data were processed using Analyst software (version 1.4.1; Applied Biosystems, Foster City, CA) in the API2000 LC-MS/MS systems.

Fifty microliters of methanol-acetic acid (100:1, v/v) was added to a 50-μl portion of the cell fraction or the cultured medium, and then the mixture was centrifuged at 17,400*g* for 10 min. The supernatant was transferred to a glass vial kept at 4°C in an autosampler, and 20 μl of this solution was injected.

Cytotoxicity Assays. An MTT assay was performed with a Cell Counting Kit-8 (Dojindo Laboratories, Kumamoto, Japan) using water-soluble [2-(2-methoxy-4-nitrophenyl)-3-(4-nitrophenyl)-5-(2, 4-disulfophenyl)-2*H*-tetrazolium monosodium salt] (WST-8). WST-8 produces a water-soluble formazan dye upon reduction in the presence of an electron carrier coupling with mitochondrial dehydrogenases. HEK/UGT cells or human hepatocytes (each 2×10^4 cell/well) were seeded in 96-well plates. After 6, 12, and 24 h of incubation for HEK/UGT cells (or after 6 h of incubation for human hepatocytes), CCK-8 reagent was added, and the absorbance of WST-8 formazan at 450 nm was measured according to the manufacturer's instructions. The percent cell viability was calculated by comparing absorbance of cells with that of the control cells.

Cell viabilities of the HEK/UGT cells and human hepatocytes were also evaluated by the intracellular ATP concentration using a CellTiter-Glo Luminescent Cell Viability Assay (Promega). The luminescence of the oxyluciferin generated was measured in the ATP assay by using an 1420 ARVO MX luminometer (excitation 338 nm and emission 458 nm) (PerkinElmer Life and Analytical Sciences–Wallac Oy, Turku, Finland) according to the manufacturer's instructions. The percent cell viability was calculated by comparing cell luminescence with that of the control cells.

Lactate dehydrogenase (LDH) leakage from HEK/UGT cells was evaluated by a Cytotoxicity Detection Kit–LDH (Roche Diagnostics GmbH, Mannheim, Germany). LDH release was measured photometrically at 490 nm (690 nm reference) according to the manufacturer's instructions. The maximum LDH release control was prepared as well as the timing of the addition of lysis solution (1% Triton X-100) to obtain 100% LDH release. The percentage of LDH release was calculated by comparing the absorbance to the maximum LDH release of the control cells.

Comet Assay. The alkaline version of the comet assay is a sensitive genotoxicity test for the detection of DNA strand breaks. The comet assay is based on the principle that DNA fragments formed via DNA damage can be detected after agarose gel electrophoresis and fluorescent staining (Singh et al., 1988). Moreover, the use of different pH conditions during the cell lysis step allows the detection of different types of DNA damage, including single- and double-strand breaks and alkali-labile sites (Kohn, 1991). The comet assay was performed as follows. In brief, HEK/UGT cells were seeded in 24-well plates 24 h before treatment. Cells were treated for 24 h with 0.5% (v/v) FBS-supplemented DMEM containing either vehicle (0.1% DMSO), 1 mM naproxen, 0.1 mM diclofenac, 1 mM ketoprofen or 1 mM ibuprofen. Microscope slides were prepared by immersion in 0.5% (w/v) normal melting agarose. One volume of cell suspension (100 μl, containing approximately 4×10^5 cells) was mixed with 9 volumes of 0.7% (w/v) low-melting point agarose maintained at 37°C in a water bath, after which 100 μl of the diluted suspension was layered on a precoated slide. The slide was immediately covered with a coverslip and incubated at 4°C to solidify the agarose. After the slides were coated with a third layer of 0.7% (w/v) low-melting point agarose at 4°C for 20 min, the embedded cells were immersed for 1 h at 4°C in cold lysis buffer [2.5 M NaCl, 1% (w/v) sodium *N*-lauroylsarcosinate, 100 mM disodium EDTA, and 10 mM Tris base, pH 10] supplemented with 1% (v/v) Triton X-100 and 10% (v/v) DMSO. The slides were placed in a horizontal electrophoresis assembly containing fresh electrophoresis buffer (100 mM NaOH and 10 mM disodium EDTA). To allow DNA unfolding and unwinding, we left the slides in the buffer for 30 min before electrophoresis. After electrophoretic resolution (300 mA for 20 min) using a recirculating horizontal tank (BE-560; Biocraft, Tokyo, Japan), the slides were washed in neutralizing buffer (0.4 M Tris-HCl, pH 7.5) twice for 5 min each and then were stained with ethidium bromide and examined in a fluorescent microscope (BZ-9000; Keyence Corporation, Osaka, Japan). The resulting photographs of fluorescently labeled comets were scored on the basis of the tail extent moment using CometAnalyzer 1.5 (Youworks Corporation, Tokyo, Japan).

The comet moment was typically determined for 150 to 180 cells per treatment on more than three separate experimental days. Data are presented as medians ± interquartile range.

Statistical Analyses. Data are expressed as the mean ± S.D. of three independent determinations. Statistical significance of the cytotoxicity data were determined by a two-tailed Student's *t* test, and comet data were analyzed using a two-tailed nonparametric Mann-Whitney's *U* test (GraphPad Software Inc., San Diego, CA). $P < 0.05$ was considered statistically significant.

Results

UGT1A3 and UGT1A4 in HEK293 Cells: Expression Levels and Enzyme Activities. To establish the stable cell line expressing UGT1A3, five clones were isolated. Immunoblot analysis revealed that the expression levels of UGT varied among the clones and the clones with the highest UGT1A protein levels were selected (data not shown). The HEK293 expression systems of UGT1A3 (HEK/

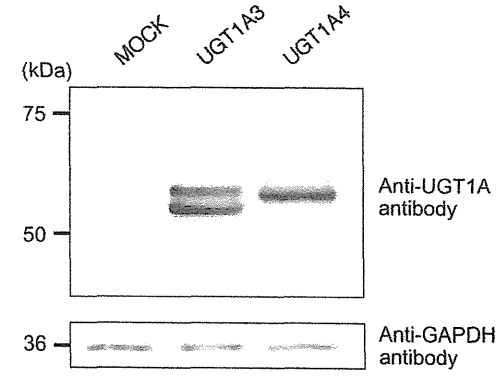

FIG. 1. SDS-PAGE and immunoblot analyses of human UGT1As proteins. Total cell homogenates from HEK/MOCK, HEK/UGT1A3, or HEK/UGT1A4 cells were prepared. The samples (10 μg) were subjected to 10% SDS-PAGE and transferred to a polyvinylidene difluoride membrane. The membrane was probed with an anti-human UGT1A antibody. The UGT1A mRNA levels were corrected with the GAPDH mRNA levels.

TABLE 1

Kinetic parameters for 4-MU O-glucuronidation by UGT1A3 and imipramine N-glucuronidation by UGT1A4 expressed in HEK293 cells

Data represent the mean ± S.D. (n = 3).

UGT Isoform	Glucuronidation	K_m	V_{max}
		mM	*pmol/(min · mg protein)*
UGT1A3	4-MU *O*-glucuronidation	0.3 ± 0.0	640.4 ± 92.1
UGT1A4	Imipramine *N*-glucuronidation	1.1 ± 0.2	240.9 ± 02.9

UGT1A3) or UGT1A4 (HEK/UGT1A4) showed a double band of approximately 54/57 kDa and a single band of approximately 56 kDa, respectively (Fig. 1). As Riedmaier et al. (2010) reported that not only UGT1A3 in human liver microsomes but also recombinant UGT1A3 appeared as a double band of approximately 54/57 kDa, the expression pattern of UGT1A3 was consistent with that of our established UGT1A3. These data indicated that the expressions of UGT1A3 and UGT1A4 were at comparable levels.

After preparation of the total cell homogenate of UGT1A3, the 4-MU *O*-glucuronidation activity was investigated. In our previous study (Fujiwara et al., 2007b), we demonstrated that the total cell homogenate of UGT1A4 could catalyze the *N*-glucuronidation of imipramine. As seen in Table 1, HEK/UGT1A3 and HEK/UGT1A4 showed enzyme activity for each substrate. These data indicated that the enzyme activity of UGT1A3 and UGT1A4 was sufficiently high.

Quantification of AG in HEK/UGT Cells. To investigate the AG formation of each stable cell line, the AG in the cell fraction and the cultured medium was quantified at 6, 12, and 24 h after treatment with the NSAIDs. The AG was not detected in HEK/MOCK and HEK/UGT1A4 cells by LC-MS/MS analysis, whereas it was detected in HEK/UGT1A3 cells (Fig. 2). The AG of naproxen, diclofenac, ketoprofen, and ibuprofen in the cell fraction at 24 h was 4.5 ± 0.8, 3.8 ± 0.4, 0.2 ± 0.1, and 7.2 ± 1.2 pmol/2 × 10^5 cells, respectively, and that in the cultured medium was 137.0 ± 0.8, 104.0 ± 13.1, 6.3 ± 0.7, and 114.7 ± 2.2 pmol/ml, respectively (Supplemental Tables 1-1 and 1-2). Compared with the AG in the cell fraction of HEK/UGT1A3, the AG in the cultured medium was increased in a time-dependent manner. The AG formed in NSAID-treated cells was not accumulated and effectively distributed in the medium.

Cytotoxicity of NSAIDs in HEK/UGT Cells. To investigate the cytotoxicity of the AGs of the NSAIDs, MTT, ATP, and LDH release assays were performed using HEK/UGT cells. In the MTT and ATP assays (Fig. 3), cell viability was decreased time dependently after treatment with the NSAIDs. However, there was no difference in the cell viability of HEK/UGT1A3 cells, which produced the AG, compared with that of HEK/MOCK and/or HEK/UGT1A4 cells. LDH leakage into the cultured medium was also assessed for 6-, 12-, and 24-h incubations. In each HEK/UGT cell line, none of the NSAIDs demonstrated LDH leakage that exceeded 5.4% of the total cell LDH levels (Supplemental Fig. 1). These results indicated that no cytotoxicity due to the AG formation from the NSAIDs was detected in HEK/UGT cells.

In addition, to investigate whether the other substrates affected the cytotoxicity, we used an MTT assay of HEK/UGT cells exposed to other carboxylic acid drugs such as clofibric acid (1 mM), gemfibrozil (1 mM), salicylic acid (1 mM), and zomepirac (0.1 mM) at 24 h. The cell viability of HEK/UGT1A3 cells was not significantly decreased compared with that of HEK/UGT1A4 cells (Supplemental Fig. 2).

Quantification of AG in Human Hepatocytes. To investigate the inhibition effect of (−)-borneol on the formation of AG in NSAID-treated human hepatocytes, the AG in the cell fraction and the cultured medium was quantified. Without (−)-borneol treatment, the AG of naproxen, diclofenac, ketoprofen, and ibuprofen formed in the cell fraction at 6 h was 33.6 ± 1.0, 59.6 ± 1.1, 6.8 ± 0.5, and 27.7 ± 1.6 pmol/2 × 10^5 cells, respectively, and that formed in the cultured medium was 1323.9 ± 44.3, 2816.1 ± 63.5, 436.8 ± 8.0, and 1156.7 ± 21.9 pmol/ml, respectively (Fig. 4). On the other hand, with (−)-borneol treatment, the AG of naproxen, diclofenac, ketoprofen, and ibuprofen formed in the cell fraction at 6 h was 10.3 ± 0.4, 15.1 ± 1.3, 1.7 ± 0.1, and 3.5 ± 0.3 pmol/2 × 10^5 cells, respectively, and that formed in the cultured medium was 393.7 ± 13.7, 610.5 ± 29.7, 54.9 ± 0.8, and 126.5 ± 10.6 pmol/ml, respectively (Fig. 4). Therefore, the AG formed in NSAID-treated human hepatocytes was decreased to one-third to one-ninth by (−)-borneol treatment.

Cytotoxicity of NSAIDs in Human Hepatocytes. We confirmed the inhibition effect of (−)-borneol on the AG formation of the NSAIDs in human hepatocytes. To investigate the effect of AG on the cytotoxicity in human hepatocytes, ATP and MTT assays were performed. In the ATP assay (Fig. 5A), the cell viability without (−)-borneol treatment was significantly decreased in the presence of the NSAIDs except ketoprofen compared with the nontreated control. If the AG showed cytotoxicity, the cell viability would be restored by (−)-borneol treatment. The cell viability with (−)-borneol treatment was further decreased, even though the AG formed in human hepatocytes was decreased. Likewise, MTT assay revealed that the cell viability was significantly decreased in the presence of naproxen (Fig. 5B). (−)-Borneol decreased the cell viability in the presence of diclofenac or ibuprofen. If the AG showed cytotoxicity, the cell viability would be restored by (−)-borneol treatment. However, (−)-borneol unexpectedly decreased the cell viability. To investigate whether the cytotoxicity is due to increased contents of the parent drugs in the cell fraction, we quantified the parent drugs using LC-MS/MS analysis. As a result, the contents of the parent drugs with (−)-borneol treatment were significantly higher than those without (−)-borneol treatment (Fig. 5C). These results indicated that the decreased cell viability of human hepatocytes with (−)-borneol treatment might be due to the increased contents of the parent drugs in the cell fraction. Therefore, AG formed in NSAID-treated human hepatocytes showed no cytotoxicity.

Comet Assay. To investigate the possibility that the AG formed in NSAID-treated HEK/UGT cells caused secondary genotoxicity by nicking DNA, the comet assay was conducted after the 24-h treatment. The scores of the tail moments of NSAID-treated HEK/UGT

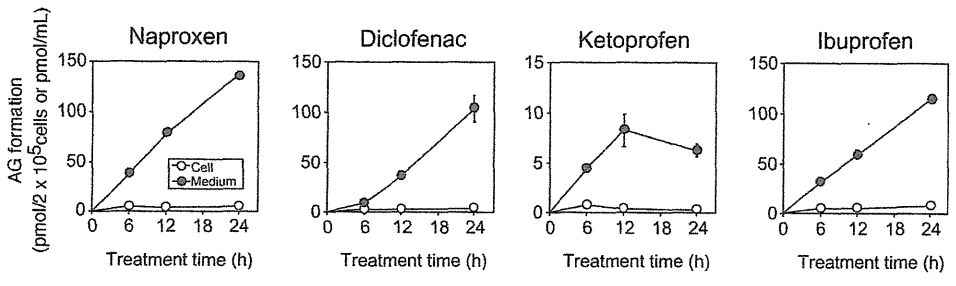

FIG. 2. Time-dependent changes of AG formation in NSAID-treated HEK/UGT1A3 cells. HEK/UGT1A3 cells (2 × 10^5 cells/ml/well) were incubated with naproxen (1 mM), diclofenac (0.1 mM), ketoprofen (1 mM), or ibuprofen (1 mM) for 6, 12, and 24 h. The cell fraction (picomoles per 2 × 10^5 cells) and the cultured medium (picomoles per milliliter) were measured by LC-MS/MS. ○, cell fraction; ●, cultured medium. Each point represents the mean ± S.D. of triplicate determinations.

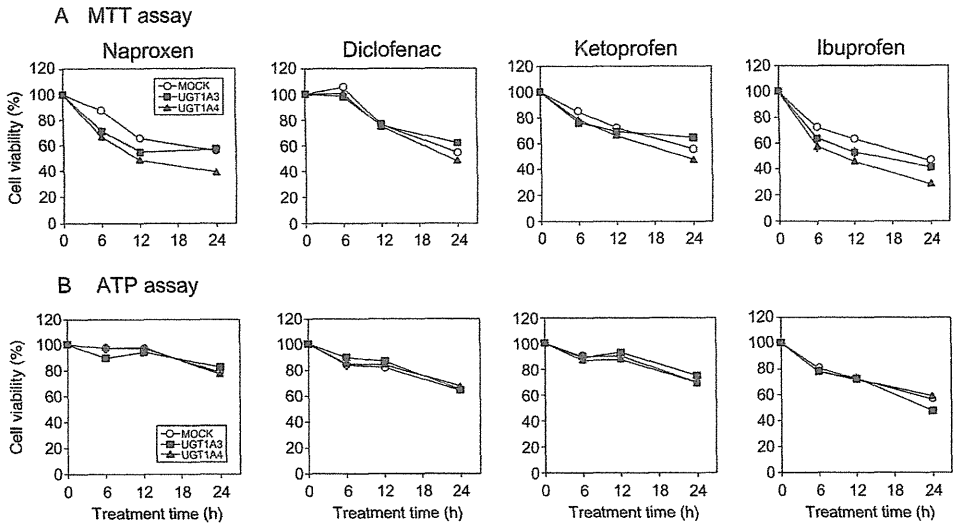

FIG. 3. Time-dependent changes of cell viability assessed by MTT and ATP assays in NSAID-treated HEK/UGT cells. A, MTT assay. B, ATP assay. HEK/UGT cells (2×10^4 cells/0.1 ml/well) were incubated with naproxen (1 mM), diclofenac (0.1 mM), ketoprofen (1 mM), and ibuprofen (1 mM) for 6, 12, and 24 h. ○, MOCK; ■, UGT1A3; ▲, UGT1A4. Each point represents the mean ± S.D. of triplicate determinations.

cells are shown in Fig. 6. Cells exposed to the NSAIDs showed hardly any DNA strand breaks compared with the controls. Methylmethane sulfonate at 0.1 mM, as a positive control, caused a significant increase in DNA migration ($P < 0.001$) compared with the solvent control (DMSO). As shown in Fig. 6B, no drugs significantly increased the DNA migration in HEK/UGT1A3 cells, even though AG was produced in the cells. No genotoxicity owing to the AG formation from the NSAIDs could be detected in the present study.

Discussion

There is increasing evidence that the formation of drug-protein adducts is involved in idiosyncratic reactions. However, direct mechanism-based evidence linking the toxicity to the formation of drug-protein adducts is lacking. We focused in this study on the toxicity due to cell dysfunction by acyl glucuronide formation. Therefore, we investigated whether the acyl glucuronide of NSAIDs represents cytotoxicity directly. In the toxicological assessment of AG in vitro, exposure of the cells to the hydrophilicity of AG must be taken into account, because it is possible that exposure to the AG from outside the cells could result in poor absorption. Therefore, to clarify the toxicity of AG, the cytotoxicity and genotoxicity of the AG formed in NSAID-treated HEK/UGT cells and human hepatocytes were evaluated at high concentrations, but there was no severe cytotoxicity from the parent drugs per se. For example, diclofenac caused low cell viability (approximately 20% of MOCK cells) at 1 mM (data not shown). Therefore, we examined diclofenac toxicity at 0.1 mM. On the other hand, naproxen, ibuprofen, and ketoprofen were examined at 1 mM.

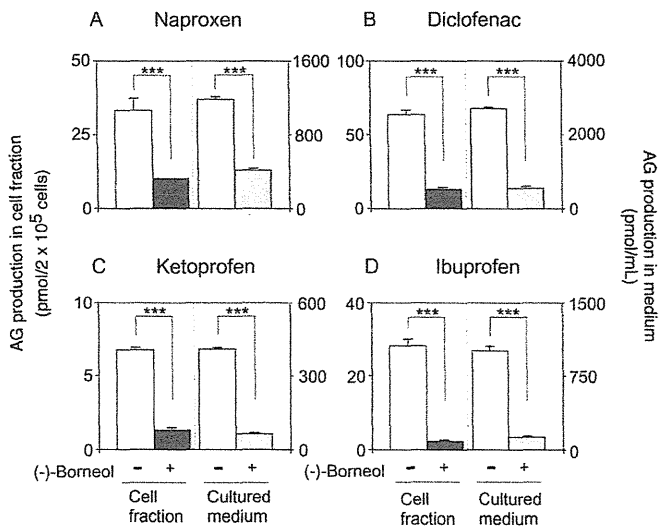

FIG. 4. Effect of (−)-borneol treatment on AG formation in NSAID-treated human hepatocytes. Human hepatocytes (2×10^5 cells/ml/well) treated with 1 mM (−)-borneol for 30 min were incubated with naproxen (1 mM) (A), diclofenac (0.1 mM) (B), ketoprofen (1 mM) (C), or ibuprofen (1 mM) (D) for 6 h. The cell fraction and the cultured medium were measured by LC-MS/MS analysis. Each point represents the mean ± S.D. of triplicate determinations. ***, $P < 0.001$ compared with without (−)-borneol treatment (control).

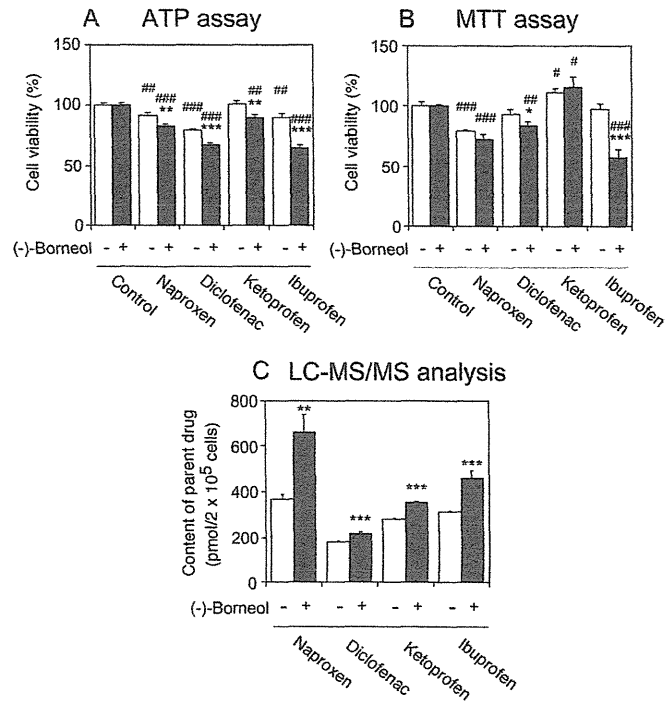

FIG. 5. Effect of (−)-borneol treatment on cell viability assessed by ATP (A) or MTT (B) assays and on contents of parent NSAIDs in the cell fraction (C) of human hepatocytes. The human hepatocytes (2×10^4 cells/0.1 ml/well) treated with 1 mM (−)-borneol for 30 min were incubated with naproxen (1 mM), diclofenac (0.1 mM), ketoprofen (1 mM), or ibuprofen (1 mM) for 6 h. □, without (−)-borneol treatment; ■, with (−)-borneol treatment. Each column represents the mean ± S.D. of triplicate determinations. *, $P < 0.05$; **, $P < 0.01$; ***, $P < 0.001$, compared with without (−)-borneol treatment. #, $P < 0.05$; ##, $P < 0.01$; ###, $P < 0.001$, compared with without NSAID treatment.

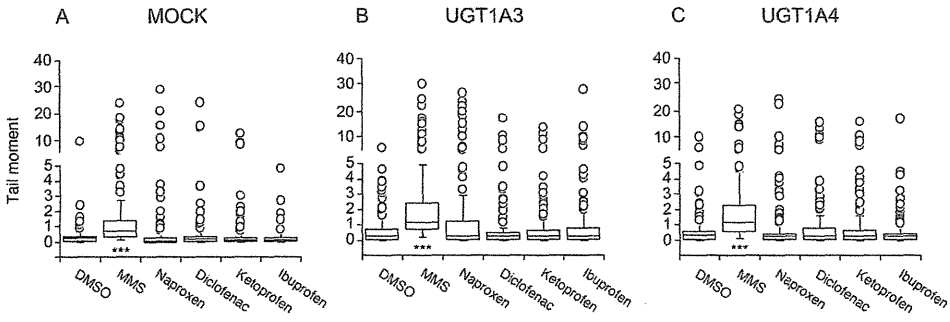

FIG. 6. DNA damage measured by the comet assay in HEK/MOCK (A), HEK/UGT1A3 (B), or HEK/UGT1A4 (C) cells. HEK/UGT cells (2×10^5 cells/ml/well) were incubated with naproxen (1 mM), diclofenac (0.1 mM), ketoprofen (1 mM), ibuprofen (1 mM), and methylmethane sulfonate (MMS) (0.1 mM, as a positive control) for 24 h. Results are shown as median (± interquartile range) tail moment calculated from 30 to 60 comets scored per slide, in more than three separate experiments (total 150–180 comets). O, outliers. ***, $P < 0.001$ compared with control (DMSO vehicle) incubations.

HEK/UGT1A3 cells were constructed to investigate the cytotoxicity of AG. HEK/UGT1A4 cells were also used as a reference for HEK/UGT1A3 cells. HEK/UGT1A4 cells have the characteristics of high amino acid homology and different catalytic properties compared with HEK/UGT1A3 cells. Moreover, HEK/UGT1A4 cells could reflect the cytotoxicity of AG more accurately than HEK/MOCK cells (Fig. 1). After exposure to the NSAIDs for 24 h, AG formation was only detected in HEK/UGT1A3 cells in a time-dependent manner (Fig. 2). However, there was no difference in the cytotoxicity to HEK/UGT1A3 cells compared with that to HEK/UGT1A4 cells, even though HEK/UGT1A3 cells could produce AG (Fig. 3; Supplemental Fig. 1). Although the cytotoxicity of other carboxylic acid drugs (i.e., clofibric acid, gemfibrozil, salicylic acid, or zomepirac) in HEK/UGT cells was investigated, the cell viability of HEK/UGT1A3 cells was not significantly decreased compared with that of HEK/UGT1A4 cells (Supplemental Fig. 2). Furthermore, the cytotoxicity of other carboxylic acid drugs such as acetylsalicylic acid, flurbiprofen, indomethacin, niflumic acid, mefenamic acid, sulindac, bezafibrate, furosemide, probenecid, or mycophenolic acid at 1 mM was investigated by using the MTT assay, and the cell viability of HEK/UGT1A3 cells was not significantly decreased (data not shown). Therefore, no cytotoxicity of AG was detected even when other carboxylic acid drugs were selected. In general, it has been thought that protein and/or DNA adduct formation in response to AG is a causal factor for toxicity. Therefore, we may not be able to exclude the possibility of increased cytotoxicity after long-term exposure to carboxylic acid drugs. To address this issue, the cytotoxicity was investigated by using the MTT assay after exposure to the drugs (naproxen, ketoprofen, ibuprofen, clofibric acid, gemfibrozil, and salicylic acid at 1 mM and diclofenac and zomepirac at 0.1 mM) for up to 72 h. However, there was no significant difference in the cell viability of the HEK/UGT cells (data not shown).

HEK293 cells have been noted to lack many uptake and efflux transporters that are normally expressed on human hepatocytes. For example, HEK293 cells do not express organic anion-transporting polypeptide 2 or 8 (Hirano et al., 2004), so that the uptake of carboxylic acid drugs may be lower than that in human hepatocytes. Likewise, HEK293 cells do not express multidrug resistance-associated protein 2 (Hagmann et al., 1999) or multidrug resistance-associated protein3 (Zeng et al., 2000), so that the efflux of intracellularly generated AG may be lower than that in human hepatocytes. Therefore, the cytotoxicity of AG was investigated by using human hepatocytes that might reflect more closely AG formation in vivo. The AG formation in human hepatocytes was much higher than that in HEK/UGT1A3 cells. In particular, the AG in the cell fraction of human hepatocytes at 6 h of treatment was approximately 6- to 30-fold that in the cell fraction of HEK/UGT1A3 cells (Figs. 2 and 4). These results suggested that other UGT isoforms (i.e., UGT1A9 and UGT2B7) catalyzing the glucuronidation of the carboxylic acid drugs and/or the transporters involved in the AG formation might be expressed in human hepatocytes. Although the AG formed in NSAID-treated human hepatocytes was decreased by (−)-borneol treatment, the cytotoxicity was increased. The LC-MS/MS analysis indicated that the content of the parent drugs in the cell fraction of human hepatocytes with (−)-borneol treatment was significantly higher than that without (−)-borneol treatment (Fig. 5C). These results suggested that the formation of AG in human hepatocytes might represent a detoxification process.

The comet assay is a unique assay method for assessing the genotoxicity of AG (Sallustio et al., 1997, 2006; Southwood et al., 2007). Thus, we investigated genotoxicity using the comet assay. The results showed that the tail moments of the DNA migration were not significantly different in the HEK/UGT cell lines, even though HEK/UGT1A3 cells produced AG in the presence of the NSAIDs. Therefore, the AG formation from the NSAIDs is not involved in genotoxicity in vitro. In a recent report, Brambilla and Martelli (2009) described the genotoxicity and carcinogenicity of many NSAIDs. According to their report, naproxen, diclofenac, ketoprofen, and ibuprofen gave negative responses in reverse mutation (Ames) tests with *Salmonella typhimurium* and in a long-term carcinogenesis assay using rats and mice. Our results showing a lack of genotoxicity for all four NSAIDs by the comet assay are in accordance with this report. On the other hand, clofibric acid (1 mM), which produced no AG metabolites, gave significantly positive results for genotoxicity by the comet assay using HEK/UGT1A3 cells at 24 h of treatment (data not shown). This result supported the previous report of Southwood et al. (2007). As described in this report, fibrate hypolipidemic agents such as clofibric acid are nongenotoxic (Ashby et al., 1994). Therefore, one should be careful in interpreting the results of the comet assay.

Among the NSAIDS containing carboxylic acid drugs, diclofenac AG is one of the most studied for its related toxicity. Diclofenac AG is excreted into bile and transported to the small intestine where it can produce erosions and ulcers in a dose-dependent manner (Seitz and Boelsterli, 1998). In a recent article, Lagas et al. (2010) reported that *Mrp2/Mrp3/Bcrp1*$^{-/-}$ mice have markedly elevated levels of diclofenac AG in their liver and display acute, albeit mild, hepatotoxicity. As for the metabolic activation, it is well known that diclofenac is converted to 4′-hydroxydiclofenac and 5-hydroxydiclofenac via direct hydroxylation and that these two metabolites are further oxidized to form benzoquinone imine intermediates by human CYP2C9 and CYP3A4, respectively (Tang et al., 1999). Quinone imines are electrophiles that have been generally implicated in redox cycling and in producing oxidative stress and can undergo covalent binding with nonprotein or protein sulfhydryl groups because of their thiol reactivity (Boelsterli, 2003). Given the toxicity of diclofenac, it seemed to be important to evaluate not only the AG but also the quinone imines of diclofenac.

In conclusion, we investigated the relationship between cytotoxicity and AG formation by NSAIDs (naproxen, diclofenac, ketoprofen, and ibuprofen) in HEK/UGT cells and human hepatocytes and also the genotoxicity of the AG from NSAIDs in HEK/UGT cells. However,